Higgs vacuum stability with vectorlike fermions

Shrihari Gopalakrishna[1,2,*] and Arunprasath Velusamy[1,†]
[1]Institute of Mathematical Sciences (IMSc), Chennai 600 113, India
[2]Homi Bhabha National Institute (HBNI), Anushaktinagar, Mumbai 400 094, India

(Received 6 February 2019; published 13 June 2019)

We present the effects of vectorlike fermions (VLFs) on the stability of the Higgs electroweak vacuum, using the renormalization group improved Higgs effective potential. We review the calculation of the one-loop beta-functions of the standard model couplings, paying particular attention to the fermion contributions. From this, we derive the VLF contributions to the beta-functions. Using these beta-functions, we determine the scale at which the effective Higgs quartic coupling becomes zero and goes negative, signaling vacuum instability. We find that for certain VLF masses and Yukawa couplings, the Higgs quartic stays positive for field values all the way up to the Planck scale, implying that the metastable vacuum of the standard model can be rendered absolutely stable if VLFs are present with certain parameters. For other values of VLF parameters, the Higgs vacuum is metastable as in the standard model. For cases where the vacuum is metastable, we compute the probability of quantum tunneling from the false electroweak vacuum into a deeper true vacuum in our Hubble volume by numerically solving for the bounce configuration in Euclidean space-time and computing the bounce action for it. We compare our numerical solution with the analytical approximation for the bounce action commonly used in the literature and comment on when the latter may be used.

DOI: 10.1103/PhysRevD.99.115020

I. INTRODUCTION

The stability of the electroweak (EW) vacuum can be studied using the Higgs effective potential (for a review, see Ref. [1]). Recent investigations (see, for example, Refs. [2–5]) at the next-to-next-to-leading order (NNLO) level have revealed that the Higgs vacuum is metastable in the standard model (SM), with the lifetime in the false (EW) vacuum being much larger than the age of the Universe. This situation arises because the Higgs quantum effective potential $V_{\rm eff}(h)$ has a smaller value for $h \sim 10^{10}$ GeV when compared to its value at the EW vacuum expectation value (VEV) $v \approx 246$ GeV, i.e., $V_{\rm eff}(h \sim 10^{10}\ \text{GeV}) < V_{\rm eff}(v)$ for the SM.

There are many compelling reasons to expect physics beyond the standard model (BSM). These include theoretical reasons such as the gauge hierarchy problem and observational reasons such as neutrino mass generation, dark matter, and generation of the baryon asymmetry of the Universe. A plethora of BSM extensions has been proposed to address these shortcomings of the SM. These inevitably add new particles to the SM particle content. In particular, resolution of the gauge hierarchy problem necessarily has new states coupled to the Higgs. In such cases, the above conclusions on Higgs EW vacuum stability must be revisited by including the effects of such new particles. Many such BSM extensions include vectorlike fermions (VLFs) that couple to the Higgs and are often the lightest BSM states. They therefore have a significant effect on EW vacuum stability. Some examples of such models that include vectorlike fermions are in the following contexts: the gauge hierarchy problem such as anti-de Sitter–space/composite-Higgs models in Refs. [6–9], Higgs-portal dark matter models in Refs. [10–14], gauge-coupling unification in Refs. [15–19], neutrino mass generation and vacuum stability in Refs. [20–25], the universal extra dimension model in Ref. [26], SM extensions with an additional $U(1)$ gauge symmetry in Refs. [27–30], models with an extended scalar sector in Refs. [31,32], a combination of these in Ref. [33–35], models of inflation in Refs. [36,37], and effective models in Refs. [38–40]. Motivated by these considerations, we study the effect of VLFs that are coupled to the Higgs on EW vacuum stability.[1] Many of these models

*shri@imsc.res.in
†arunprasath@imsc.res.in

[1]New chiral (fourth generation) fermions that get their mass from the Higgs are severely disfavored with a single Higgs doublet from the recent LHC Higgs cross section and couplings measurements. In contrast, VLFs tend to have milder constraints on them, owing to their nice decoupling property.

may also contain new bosonic states apart from VLFs. In such a case, a full conclusion about the stability of the EW vacuum in that model can be reached only after including the contributions of these bosonic states also. However, fermions usually have the biggest role in destabilizing the EW vacuum, and so our analysis here addresses the most crucial ingredient in this problem. Hence, our goal here is to analyze model independently the generic effects of VLFs on EW vacuum stability.

We set the stage for our analysis by writing the classical Higgs potential as

$$\mathcal{V} = \frac{m_h^2}{2}h^2 + \frac{\lambda}{4}h^4. \tag{1}$$

Including quantum effects, we can write the quantum Higgs effective potential as

$$V_{\rm eff}(h) = \frac{m_{h\rm eff}^2}{2}h^2 + \frac{\lambda_{\rm eff}(h)}{4}h^4, \tag{2}$$

where $\lambda_{\rm eff}$ has a dependence on h of the form $\ln(h/M)$ with M being a subtraction scale. For $h \gg m_h$ (the physical Higgs mass $m_h \approx 125$ GeV), the mass term has a negligible effect, and thus, to an excellent approximation, we can write

$$V_{\rm eff}(h) = \frac{\lambda_{\rm eff}(h)}{4}h^4. \tag{3}$$

Denoting the field value as $h \equiv \mu$ and denoting $\lambda_{\rm eff}(\mu)$ as just $\lambda(\mu)$, it can be shown (see, for example, Ref. [41]) that $\lambda(\mu)$ obeys a renormalization group equation (RGE) of the form

$$\frac{d\lambda(\mu)}{d\ln\mu} = \beta_\lambda(\lambda(\mu), y_t(\mu), g_3(\mu), g_2(\mu), g_1(\mu), \ldots). \tag{4}$$

The RGE is interpreted now as an evolution with field value $h = \mu$, and the β-function β_λ is the usual β-function for the coupling λ, governed by the RGE. The $\lambda(\mu)$ obtained by integrating the RGE has the leading logs of the form $\log^n(\mu/M)$ resummed. β_λ is shown as a function of λ itself and also of the other couplings that contribute significantly, which, in the SM, are the top Yukawa coupling y_t and the $SU(3)$, $SU(2)$, and $U(1)$ gauge couplings $g_a = \{g_3, g_2, g_1\}$. All these couplings also evolve with μ via analogous RGE equations with their corresponding β-functions β_{y_t}, β_{g_a}. We neglect the contributions of the other SM couplings to the β-functions as they contribute insignificantly. From Eq. (3), we see that for $h \gg m_h$, the instability is signalled by the Higgs quartic effective coupling $\lambda(\mu)$ becoming negative.

As we show explicitly later, β_λ obtains a negative contribution from y_t, while it obtains a positive contribution from $\lambda(\mu)$ itself and from gauge couplings. Thus, the top quark has the important effect of decreasing $\lambda(\mu)$, and for y_t as large as in the SM, for the observed m_h, it drives $\lambda(\mu)$ negative at higher energies, signaling vacuum instability. The effect of fermions coupled to the Higgs is generally to destabilize the electroweak vacuum, although in this work, we show that this statement is not so definite. Many extensions beyond the SM include new fermions, and the question we address in this work is what the effects of new fermions might be on Higgs vacuum stability in light of the observation made above.

The subject of this work is to include VLF contributions to the β-functions and find the consequences for EW vacuum stability and how it is changed from the SM. We ask if $\lambda(\mu)$ still becomes zero with VLF present, and if so at what μ, and compare it with the SM case. If the vacuum is unstable, we compute the tunneling probability to ascertain if it decays within the age of the Universe, in which case it is unacceptable. On the contrary, if the lifetime in the EW vacuum is comparatively much larger than the age of the Universe, it is metastable and phenomenologically acceptable. To this end, we study some simple VLF extensions of the SM, where the VLFs are either in the trivial or fundamental representations of $SU(3)$, $SU(2)$, and $U(1)$, and demonstrate their effects on Higgs vacuum stability. In particular, the VLFs we add are of two kinds, namely, $SU(3)$ triplet vectorlike quarks (VLQ) and $SU(3)$ singlet vectorlike leptons (VLLs).

The paper is organized as follows. In Sec. II, we list the one-loop RGE in the SM and include some significant two-loop corrections from the literature. We present a derivation of the fermionic contributions to the RGE in Appendix A. We then derive the one-loop VLF contributions to the RGE and add these to the SM RGE. We present the calculational details of the VLF contributions in Appendix B. We integrate the RGE numerically and show the evolution of the couplings as a function of the field value $h \equiv \mu$. In Sec. III, we compute the probability that our electroweak vacuum would have tunneled into a deeper true vacuum in our Hubble volume in the case where the EW vacuum is metastable. We do so by solving for the bounce configuration numerically and computing the Euclidean action for this. In Sec. IV, we make some remarks for the case when the VLFs render the EW vacuum absolutely stable. In Sec. V, we compare our numerical evaluation of the bounce action to an approximation commonly used in the literature and provide a cautionary note on when the approximation can be applied. We offer our conclusions in Sec. VI.

II. RENORMALIZATION GROUP IMPROVED HIGGS EFFECTIVE POTENTIAL

We have in the SM the Lagrangian density, showing only the terms relevant to our analysis here,

$$\mathcal{L} \supset \bar{t}i\partial\!\!\!/ t - \lambda(H^\dagger H)^2 - (y_t \bar{q}_L \cdot H^* t_R + \text{H.c.}), \tag{5}$$

where the $\cdot$ represents the antisymmetric combination in $SU(2)$ space, $q_L = (t_L b_L)^T$ is the $SU(2)$ doublet, and $t = (t_L t_R)^T$ and $b = (b_L b_R)^T$ are the top-quark and bottom-quark Dirac fermions. It is sufficient for our purposes to keep only the top Yukawa coupling y_t in the SM as the others are very suppressed. Next, we present the SM β-functions and extend them to include the VLF contributions.

A. SM RGE

We first discuss the SM RGE β-functions at the one-loop level and include some significant two-loop effects. We use the SM RGE to find the Higgs field value at which $\lambda(\mu)$ becomes zero and compare our results with those in the literature. Denoting the relevant SM couplings generically as $\kappa_i = \{\lambda, y_t, g_3, g_2, g_1\}$, the RGE are of the form

$$\frac{d\kappa_i(\mu)}{d\ln\mu} = \beta_{\kappa_i}(\kappa_j(\mu)). \tag{6}$$

We derive the fermion contributions to β_κ in Appendix A since our goal in this work is to extend them to include VLF contributions. We take the other terms from the literature (see, for example, Ref. [4]). Putting these together, the one-loop β-functions, $\beta_\kappa^{(1)}$, are

$$\beta_\lambda^{(1)} = \frac{1}{16\pi^2}\left[24\lambda^2 + 4N_c y_t^2\lambda - 2N_c y_t^4 - 9g_2^2\lambda - \frac{9}{5}g_1^2\lambda + \frac{9}{8}\left(g_2^4 + \frac{2}{5}g_2^2 g_1^2 + \frac{3}{25}g_1^4\right)\right], \tag{7}$$

$$\beta_{y_t}^{(1)} = \frac{y_t}{16\pi^2}\left[\frac{(3+2N_c)}{2}y_t^2 - 8g_3^2 - \frac{9}{4}g_2^2 - \frac{17}{20}g_1^2\right], \tag{8}$$

$$\beta_{g_a}^{(1)} = \frac{g_a^3 b_a}{16\pi^2}, \tag{9}$$

with $b_a = (-7, -19/6, 41/10)$ for $g_a = (g_3, g_2, g_1)$, respectively, and $N_c = 3$ for a fermion in the fundamental representation of $SU(3)$. For g_1, we use the $SU(5)$ normalization; i.e., the SM hypercharge gauge-coupling g' is related to g_1 by $g_1 = \sqrt{5/3}g'$.

The precision of the full two-loop (or higher order) calculations that are available in the literature are not required for our purposes since our goal is to analyze BSM physics contributions that involve as yet experimentally undetermined parameters. However, to help compare our numerical results to what has been obtained in the literature for the SM, we will include two-loop SM contributions to the β-functions that depend on y_t and g_3 as they are numerically the most significant. They are (see, for example, Ref. [4])

$$\beta_\lambda^{(2)} = \frac{y_t^2}{(16\pi^2)^2}(30y_t^4 - 32g_3^2y_t^2 + 80\lambda g_3^2 + \cdots), \tag{10}$$

$$\beta_{y_t}^{(2)} = \frac{y_t}{(16\pi^2)^2}\left[\left(-\frac{404}{3} + \frac{40}{9}n_3^{(\mathrm{SM})}\right)g_3^4 + 36y_t^2g_3^2 - 12y_t^4 + \cdots\right], \tag{11}$$

$$\beta_{g_3}^{(2)} = \frac{g_3^3}{(16\pi^2)^2}\left[(-86 + 10n_3^{(\mathrm{SM})})g_3^2 - 2y_t^2 + \cdots\right], \tag{12}$$

where $n_3^{(\mathrm{SM})} = 6$ is the number of $SU(3)$-triplets (i.e., quarks) in the SM.

We use these RGEs to determine the Higgs field value μ at which $\lambda(\mu)$ becomes zero, signalling vacuum instability. This will be discussed in Sec. II C. We discuss next the VLF contributions to the RGE.

B. VLF contributions to the RGE

We add an $SU(2)$ doublet VLF $\chi = (\chi_1\chi_2)^T$ and an $SU(2)$ singlet VLF ξ and couple it to the Higgs as follows,

$$\mathcal{L} \supset -M_\chi\bar{\chi}\chi - M_\xi\bar{\xi}\xi - (\tilde{y}\,\bar{\chi}\cdot H^*\xi + \mathrm{H.c.}), \tag{13}$$

where the $\cdot$ represents the antisymmetric combination in $SU(2)$ space.[2] Extracting the Higgs interactions from this yields

$$\mathcal{L} \supset -\frac{\tilde{y}}{\sqrt{2}}h(\bar{\chi}_1\xi + \bar{\xi}\chi_1). \tag{14}$$

If χ and ξ have color $N_c' = 3$, we call them vectorlike quarks (VLQs), and if they are trivial under $SU(3)$, i.e., $N_c' = 1$, we call them vectorlike leptons. The $SU(3)$, $SU(2)$, and $U(1)$ gauge interactions are standard, and we do not show them explicitly. We denote the hypercharge of χ as Y_χ, that of ξ as Y_ξ, and that of the Higgs doublet is $Y_H = 1/2$ as in the SM. If $N_c' = 3$, the VLQs have gluon interactions, while if $N_c' = 1$, the VLLs do not have gluon interactions.

For SM-like choices of Y_χ and Y_ξ, mixed Yukawa couplings between the VLF and the standard model fermions (SMFs) can be written down. However, collider, flavor changing neutral current, and other precision constraints restrict how large such couplings can be (for details, see, for example, Ref. [42]). For simplicity, in this work, we do not turn on such mixed Yukawa couplings; an analysis

[2]If another $SU(2)$ singlet VLF ζ is added, we can add the terms $\mathcal{L} \supset -M_\zeta\bar{\zeta}\zeta - (\tilde{y}_2\bar{\chi}H\zeta + \mathrm{H.c.})$. After adding the ζ, the one doublet and two singlet VLF structure then mimics the SM quark or lepton structure in a generation. For keeping the field content minimal, we will omit the ζ in our work here and therefore will not include the $\tilde{y}_2$ term.

including such mixed couplings will be the subject of future work.

We derive the one-loop RGE contributions due to the VLF (see Appendix B for the derivation) and add them to the SM contributions given above. The VLF contributions to the RGE in Eqs. (7)–(9) and the SM and VLF contributions to the RGE for the new coupling $\tilde{y}$ are

$$\beta_{g_3}^{(1)\mathrm{VLF}} = \frac{g_3^3}{16\pi^2}\left(\frac{2}{3}n_3\right), \tag{15}$$

$$\beta_{g_2}^{(1)\mathrm{VLF}} = \frac{g_2^3}{16\pi^2}\left(\frac{2}{3}N_c' n_2\right), \tag{16}$$

$$\beta_{g_1}^{(1)\mathrm{VLF}} = \frac{g_1^3}{16\pi^2}\left[\frac{4}{5}N_c'(2n_2 Y_\chi^2 + n_1 Y_\xi^2)\right], \tag{17}$$

$$\beta_{\lambda}^{(1)\mathrm{VLF}} = \frac{2n_F}{16\pi^2}(4N_c'\tilde{y}^2\lambda - 2N_c'\tilde{y}^4), \tag{18}$$

$$\beta_{y_t}^{(1)\mathrm{VLF}} = \frac{n_F}{16\pi^2}y_t(2N_c'\tilde{y}^2), \tag{19}$$

$$\beta_{\tilde{y}}^{(1)} = \frac{\tilde{y}}{16\pi^2}\left[\frac{(3\tilde{y}^2 + 2N_c y_t^2 + 4n_F N_c'\tilde{y}^2)}{2} - 8\hat{n}_F^{\mathrm{VLQ}} g_3^2 - \frac{9}{4}g_2^2 - \frac{9}{5}g_1^2(Y_H^2 + 2Y_\chi Y_\xi)\right], \tag{20}$$

where n_3 is the number of colored VLF $SU(3)$ triplets, i.e., VLQs; n_2 is the number of $SU(2)$ doublets; n_1 is the number of $SU(2)$ singlets; n_F is the number of complete VLF families coupled to the Higgs (a family is a doublet and a singlet *both* present); and $\hat{n}_F^{\mathrm{VLQ}} = 1$ if the VLF is a VLQ family or zero otherwise. For example, $n_F = 0$ for either VLF singlets or doublets added (but not both), and $n_F = 1$ for one $SU(2)$ doublet and one singlet VLF added together such that a Yukawa coupling $\tilde{y}$ can be written down with the Higgs. Only VLQs contribute to β_{g_3}, and VLLs do not. For instance, for one VLQ family of χ and ξ, we have $N_c' = 3$, $n_3 = 3$, $n_2 = 1$, $n_1 = 1$, $n_F = 1$, and $\hat{n}_F^{\mathrm{VLQ}} = 1$.

To improve precision, we include the dominant two-loop VLF contributions to the β-functions obtained from the package SARAH [43,44], which are

$$\beta_{g_3}^{(2)\mathrm{VLF}} = \frac{g_3^3}{(16\pi^2)^2}(10n_3 g_3^2 - 2\times 2\hat{n}_F^{\mathrm{VLQ}}\tilde{y}^2 + \cdots), \tag{21}$$

$$\beta_{\lambda}^{(2)\mathrm{VLF}} = \frac{\tilde{y}^2 n_F}{(16\pi^2)^2}(2\times 10N_c'\tilde{y}^4 - 2\times 32\hat{n}_F^{\mathrm{VLQ}} g_3^2\tilde{y}^2 + 2\times 80\hat{n}_F^{\mathrm{VLQ}}\lambda g_3^2 + \cdots), \tag{22}$$

$$\beta_{y_t}^{(2)\mathrm{VLF}} = \frac{y_t}{(16\pi^2)^2}\left(\frac{40}{9}n_3 g_3^4 - \frac{9}{2}n_F N_c'\tilde{y}^4 - \frac{9}{2}n_F N_c'\tilde{y}^2 y_t^2 + 40n_F^{\mathrm{VLQ}} g_3^2\tilde{y}^2 + \cdots\right), \tag{23}$$

$$\beta_{\tilde{y}}^{(2)} = \frac{\tilde{y}}{(16\pi^2)^2}\left[-\left(9N_c' - \frac{3}{2}\right)\tilde{y}^4 + \hat{n}_F^{\mathrm{VLQ}}\left(-\frac{2\times 485}{9} + \frac{40}{9}(n_3^{(\mathrm{SM})} + n_3)\right)g_3^4 + 56\hat{n}_F^{\mathrm{VLQ}}\tilde{y}^2 g_3^2 + 20 g_3^2 y_t^2 - \frac{27}{4}\tilde{y}^2 y_t^2 - \frac{27}{4}y_t^4 + \cdots\right], \tag{24}$$

where n_F^{VLQ} is the number of colored families, and as noted earlier, $n_3^{(\mathrm{SM})} = 6$. We have explicitly checked that the above dominant contributions closely reproduce numerically the full two-loop running from SARAH.

Our goal in this work is to analyze the stability of the EW vacuum for which the behavior of V_{eff} at large field values is most important. We have therefore not kept the finite mass effects in the RGE as they are small, being of the form (m/μ) for $\mu \gg m$ where m collectively denotes the particle masses. We include the VLF contributions only for $\mu \geq M_{VL}$, where M_{VL} is the vectorlike fermion mass.

C. RGE Numerical integration results

We take the input parameters as follows and as compiled in Ref. [4], with the renormalization point taken as the top mass scale $\tilde{m}_t$:

- the EW VEV: $v = 246.2$ GeV,
- the Higgs quartic: $\tilde{\lambda} = 0.12710$ (NNLO),
- the top Yukawa coupling: $\tilde{y}_t = 0.93558$ (partial three-loop),
- the $SU(3)_c$ coupling constant: $\tilde{g}_3 = 1.1666$ (partial four-loop),
- the $SU(2)_L$ coupling constant: $\tilde{g}_2 = 0.64755$ (next-to-leading order),
- the $U(1)$ coupling constant: $\tilde{g}_1 = \sqrt{5/3}\tilde{g}' = \sqrt{5/3}\times 0.35937$ (next-to-leading order).

In terms of these inputs, we set the top mass to be $\tilde{m}_t = \tilde{y}_t v/\sqrt{2}$ and the Higgs mass $\tilde{m}_h = \sqrt{2\tilde{\lambda}}v$. In this work, since our interest is in analyzing a new physics (VLF) model with unknown parameters, the full precision to which these are defined is not so important, and the above specification is more than adequate for our purposes.

The RGEs are a coupled set of first order differential equations for the couplings $\lambda(\mu)$, $y_t(\mu)$, $g_3(\mu)$, $g_2(\mu)$, and $g_1(\mu)$. We take the inputs given above at $\tilde{m}_t$ and integrate the RGE numerically, including both the SM contributions in Sec. II A and the VLF contributions in Sec. II B. As already mentioned, we include the VLF contribution only for $\mu \geq M_{VL}$.

In Figs. 1–4 we show the evolution of the different couplings for the SM and also for some representative VLF cases. In these figures, the dashed lines are for the SM with only the SM particle content with no VLFs, while the solid lines are for various VLF cases. As is evident, in the SM, all the couplings decrease with field value $h \equiv \mu$. The Higgs quartic coupling λ becomes zero and goes negative at about $\mu \sim 10^{10.5}$ GeV, while all the other couplings stay positive all the way up to $M_{\rm Pl}$. It is interesting that β_λ approaches zero for large field values (cf. Fig. 9). In the following, we discuss the evolution of the couplings in the presence of VLFs.

In Fig. 1, we show the evolution of the couplings with field value $h \equiv \mu$ for (n) degenerate $SU(2)$ singlet VLQs for various M_{VL}, where the M_{VL} values are shown in the notation $(rEm) \equiv r \times 10^m$ GeV. When three or more degenerate singlet VLQs of mass 3 TeV are added, interestingly, λ never goes negative, unlike in the SM. When we add only singlet VLQs, $SU(2)$ invariance forbids a coupling of the Higgs to such VLQs, (we do not turn on mixed Yukawa couplings between SM fermions and VLFs as we noted earlier). However, these VLQs contribute to β_{g_3} and also to β_{g_1} if the VLQ has hypercharge, and because of the coupled nature of the RGEs, $\lambda(h)$ does see the effect of the VLQ. In particular, even if $\tilde{y}$ is very small, the VLQ contribution to β_{g_3} given in Eq. (15) still remains and, being positive, results in $g_3(\mu)$ being larger for larger μ as compared to the SM. A larger g_3 means that the second term in Eq. (8) is more negative, causing the $y_t(\mu)$ to be smaller in comparison to the SM case. A smaller y_t implies a less negative contribution to β_λ from the third term of Eq. (7), which means that the $\lambda(\mu)$ is larger with VLQs present. For large enough n_3, this results even in a turn around to a positive β_λ, allowing for the possibility of λ never going negative. We discuss the implications of this to vacuum stability in Sec. IV.

In Fig. 2, we show the evolution of the couplings with field value $h \equiv \mu$ for (n) degenerate $SU(2)$ doublet VLQs for various M_{VL}. We observe that when we add one or more doublet VLQs of mass 3 TeV, λ never goes negative for the same reasons as above. We also see that adding a doublet VLQ with mass up to about 10^5 GeV will have this feature. We discuss in Sec. IV the implications to vacuum stability of λ remaining positive. If we add five or more doublets with 3 TeV mass, we find that, due to the large positive VLF contribution to β_{g_2} given in Eq. (16), g_2 grows and becomes nonperturbative at $\mu \approx 10^{16}$ GeV, invalidating this perturbative analysis at around that scale. In Fig. 2, we have restricted the five doublet curves to the region $g_2 < 10$ so that our perturbative analysis is reliable. The negative contribution proportional to g_2^2 in β_{y_t} given in Eq. (8) becomes significant as g_2 becomes large and leads to a smaller y_t. Also, β_{g_3} gets a large positive VLF contribution from Eq. (15) causing g_3 to increase with μ.

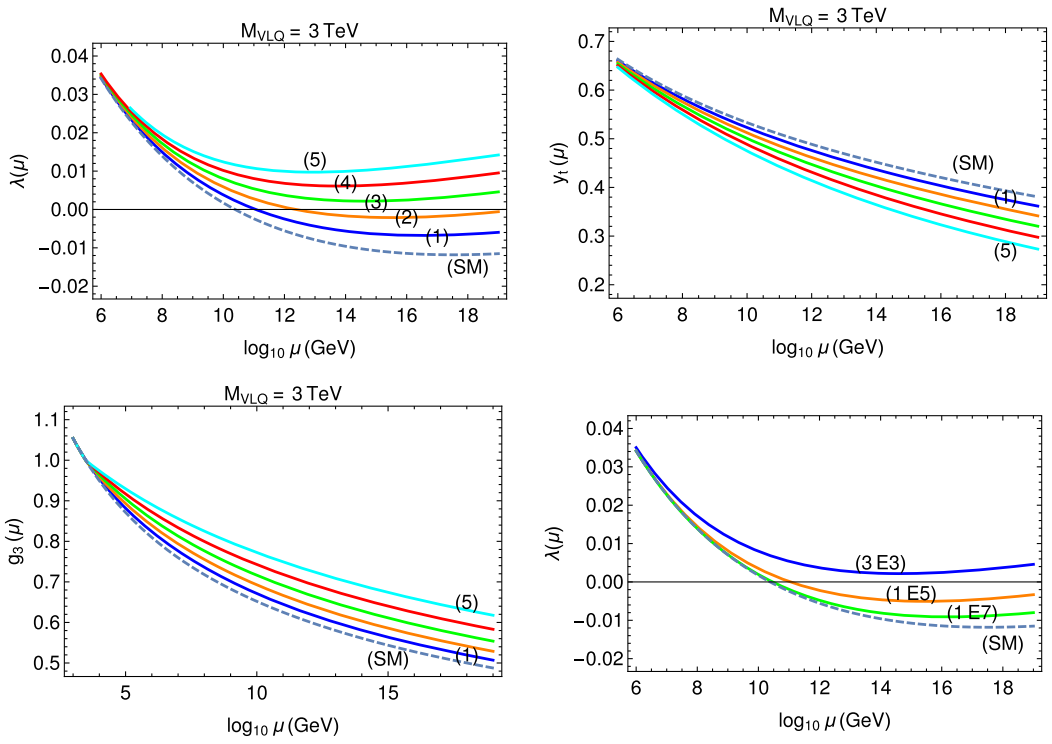

FIG. 1. The evolution of λ, y_t, and g_3 with Higgs field value μ for (n) number of degenerate $SU(2)$ singlet VLQs of mass 3 TeV (first three plots) and λ with three degenerate singlet VLQs of mass 3×10^3 GeV, 10^5 GeV, and 10^7 GeV shown, respectively, as $3E3$, $1E5$, and $1E7$ (last plot).

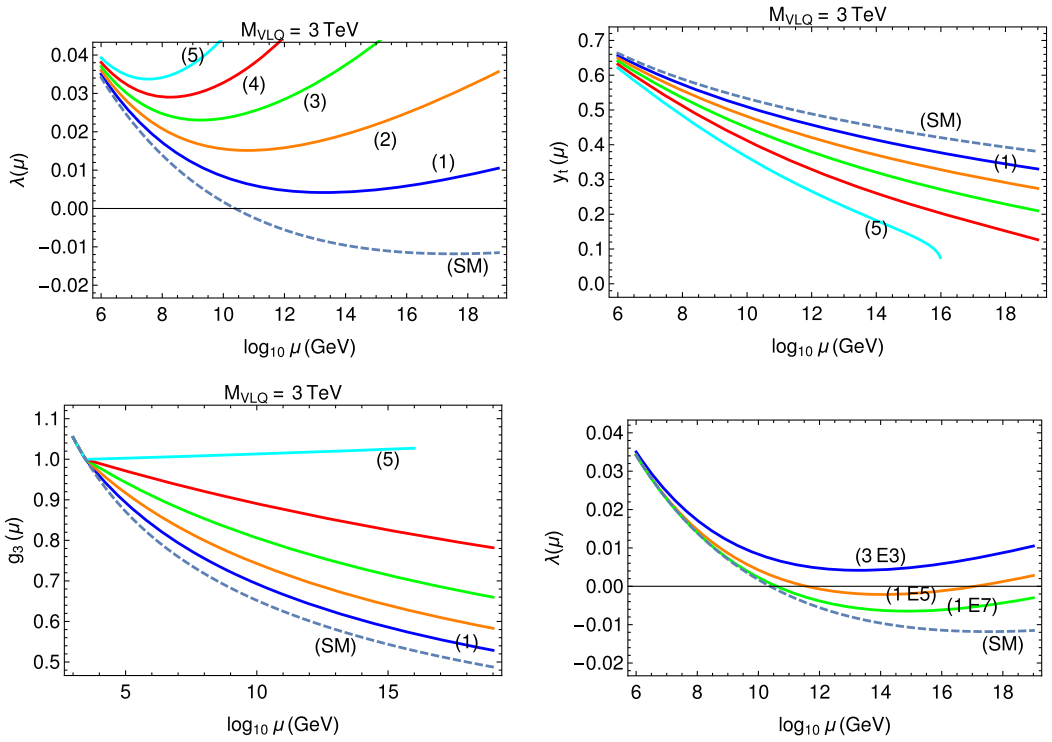

FIG. 2. The evolution of λ, y_t, and g_3 with the Higgs field value μ for (n) number of degenerate $SU(2)$ doublet VLQs of mass 3 TeV (first three plots) and λ with a doublet VLQ of mass 3×10^3 GeV, 10^5 GeV, and 10^7 GeV shown, respectively, as $3E3$, $1E5$, and $1E7$ (last plot).

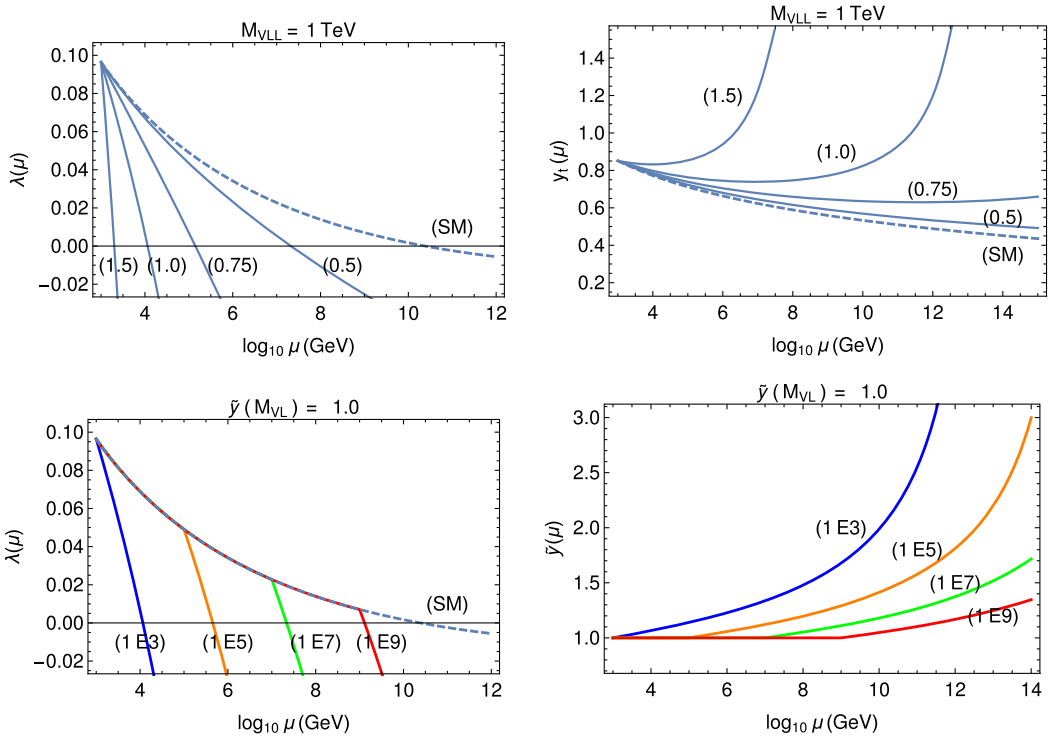

FIG. 3. The evolution of λ, y_t, and $\tilde{y}$ with Higgs field value μ for a degenerate family of one $SU(2)$ doublet VLL and one singlet VLL, for $M_{VL} = 1$ TeV and various $\tilde{y}$ (first two plots) and for $\tilde{y}(M_{VL}) = 1$ and various M_{VL} (in GeV) (last two plots).

In Fig. 3, we show the evolution of the couplings with field value $h \equiv \mu$ for a degenerate family of one $SU(2)$ doublet VLL and one singlet VLL for various M_{VL} and $\tilde{y}$. The VLL Yukawa coupling values are shown as $(\tilde{y})$, and the M_{VL} values are shown in the notation $(rEm) \equiv r \times 10^m$ GeV. For $\tilde{y}(M_{VL}) = 1$, we see that $\tilde{y}$ increases as μ increases. y_t eventually starts increasing at large μ, which is a behavior unlike in the SM. We notice that the scale at which λ becomes negative decreases as $\tilde{y}$ increases, or as M_{VL} decreases.

In Fig. 4, we show the evolution of the couplings with field value $h \equiv \mu$ for a degenerate family of one $SU(2)$ doublet VLQ and one singlet VLQ, for various M_{VL} and $\tilde{y}$. We see that for $\tilde{y}(M_{VL}) = 0.5$, $\tilde{y}$ decreases as μ increases. For $M_{VL} = 3$ TeV, if $\tilde{y} > 0.35$, the scale at which λ becomes negative decreases as $\tilde{y}$ increases or as M_{VL} decreases and is lesser than in the SM, while if $\tilde{y} < 0.35$, the scale at which λ becomes negative is larger than in the SM. In fact, for $\tilde{y} < 0.3$, λ stays positive all the way up to $M_{\rm Pl}$. We see that when $\tilde{y} = 0.1$ for example, λ stays positive all the way up to $M_{\rm Pl}$ for M_{VL} up to about 10^5 GeV.

These examples illustrate a range of effects on the evolution of the couplings due to VLFs. For the cases when λ does go negative, the EW vacuum is not the absolute minimum but is metastable. There is then a nonzero probability that the EW vacuum will tunnel quantum mechanically away to those (large) field values where $V_{\rm eff} < 0$. We turn next to an analysis of this possibility and a computation of the tunneling probability.

III. TUNNELING AWAY FROM EW VACUUM

In this section, we compute the tunneling probability from the metastable electroweak Higgs vacuum into a

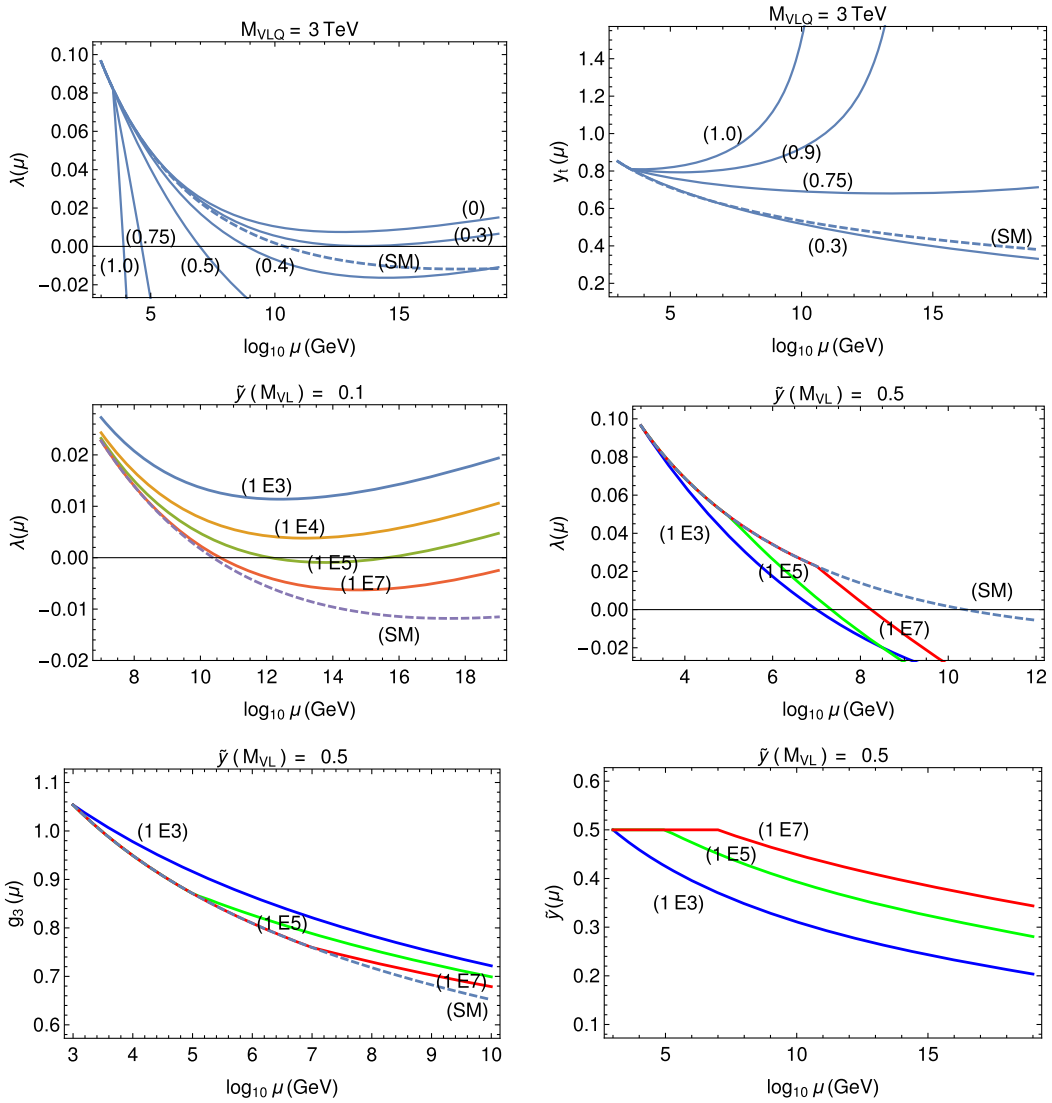

FIG. 4. The evolution of λ, y_t, g_3, and $\tilde{y}$ with Higgs field value μ for a family of one $SU(2)$ doublet VLQ and one singlet VLQ for various M_{VL} and $\tilde{y}$. The top row is for $M_{\rm VLQ} = 3$ TeV, while the bottom row is for different M_{VL} (in GeV) for $\tilde{y}(M_{VL}) = \{0.1, 0.5\}$.

deeper true vacuum via quantum mechanical barrier penetration. We do this by computing the *Euclidean action* for the *bounce* configuration of the Higgs field (for a review, see, for example, Ref. [45]). We compute the bounce configuration using the running couplings that we presented in Sec. II. From the bounce action S_B, we compute the tunneling probability P_{tunl}.

A. Method of computing the tunneling probability

We briefly review here how to compute the bounce configuration and the tunneling probability (for details, see, for example, Refs. [1,45] and references therein). In Sec. V, we discuss in detail why we do not use the approximation commonly used in the literature but resort to actually solving the bounce equation of motion (EOM) numerically as described in this section.

Let us recall that the Lagrangian density $\mathcal{L}$ and the *action* S for the Higgs field in Minkowski coordinates are

$$\mathcal{L} = \frac{1}{2}\partial^\mu h \partial_\mu h - V_{\rm eff}(h); \quad S = \int d^4x \mathcal{L}, \tag{25}$$

with the effective potential defined in Eq. (2). We define the Euclidean time $\tau = it$, the Euclidean coordinates $\rho^i = \{\tau, x^1, x^2, x^3\}$ with $i = \{1, 2, 3, 4\}$, and the invariant $\rho^2 = \tau^2 + (x^1)^2 + (x^2)^2 + (x^3)^2$ and write the Euclidean action as

$$S_E = \int d^4\rho \left[\frac{1}{2}(\partial_i h)^2 + V_{\rm eff}(h)\right], \tag{26}$$

where ∂_i is with respect to the Euclidean coordinates ρ^i.

As mentioned earlier, taking $V_{\rm eff}(v) = 0$ at the EW minimum, the central question of interest in our work here is whether the EW vacuum is absolutely stable or if there is a possible transition to other field values, which would be possible only if $V_{\rm eff}(h) < 0$ for some h typically much larger than v. If there exists field values for which $V_{\rm eff}(h) < 0$, the EW vacuum at $h = v$ is typically separated from this by a (large) barrier and a vacuum transition can only occur via quantum tunneling. In such a situation, we would like to know the timescale of the tunneling in comparison to the age of the Universe and see if we can gain an understanding of why the Universe has not tunneled away to the true vacuum with $h \gg v$ but is in the EW vacuum today. If for some large field value, $h \equiv \sigma$ say, suppose $V_{\rm eff}(\sigma) = 0$, and suppose $V_{\rm eff}$ is negative for $h \gtrsim \sigma$. [$V_{\rm eff}$ may turn around and have a second minimum (or not) for $h > \sigma$ depending on other BSM contributions in the RGE]. Equivalently, from our definition of the field dependent coupling in Eq. (3), suppose $\lambda(\sigma) = 0$ and that $\lambda(h)$ is negative for $h \gtrsim \sigma$. The vacuum configuration defined to have total energy $E = 0$ at $h = v$ can quantum mechanically tunnel to $h \geq \sigma$ with $V_{\rm eff}(h) < 0$. If the vacuum were to tunnel so, the field then runs down the potential classically toward large field values $h > \sigma$. The tunneling probability is given in terms of the bounce configuration [45], which satisfies $\delta S = 0$, starting with $h(t = -\infty) = v$, attaining a value $h(t = 0) \equiv h_0 \geq \sigma$, and returning to $h(t = \infty) = v$. This configuration is a solution of the EOM. In Euclidean coordinates, the EOM reads

$$\partial_i^2 h = \frac{\partial V_{\rm eff}}{\partial h}. \tag{27}$$

We look for an $O(4)$ symmetric solution [46], which implies that it depends on ρ, i.e., $h(\rho^i) = h(\rho)$. The EOM then reads

$$\frac{d^2h}{d\rho^2} + \frac{3}{\rho}\frac{dh}{d\rho} = \frac{\partial V_{\rm eff}}{\partial h}, \tag{28}$$

with the boundary conditions (BCs) $(dh/d\rho)(\rho = 0) = 0$ and $h(\rho \to \infty) = v$. We must also have $h(\rho = 0) = h_0 \geq \sigma$ for this to represent tunneling. This EOM is identical to that of a classical particle moving in a potential $-V_{\rm eff}$ with a "friction" term present [second term in Eq. (28)] that dies off as $1/\rho$ as ρ increases.

In Euclidean space-time, the bounce configuration $h_B(\rho)$ will have the feature of a fairly sharp transition in ρ from h_0 to v. In Minkowski space-time, this configuration looks like an expanding bubble with the bubble wall separating a region of true vacuum inside and the false EW vacuum outside. The bubble nucleation probability per unit 4-volume is given by [1] $\Delta P_{\rm tunl}/\Delta V_4 = M^4 \exp(-S_B)$, where we have included a prefactor of M^4 on dimensional grounds with M an appropriate mass scale, ΔV_4 is a unit 4-space-time volume, and S_B is the Euclidean action for the bounce configuration $h_B(\rho)$ given by

$$S_B = 2\pi^2 \int_0^\infty d\rho \rho^3 \left[\frac{1}{2}\left(\frac{dh_B}{d\rho}\right)^2 + V_{\rm eff}(h_B)\right]. \tag{29}$$

We make the choice $M^4 = V_{\rm eff}(h_0)$ since h_0 is typically the largest scale in the problem and gives the largest tunneling rate and hence the most conservative bound on the allowed VLF parameter space from vacuum tunneling.

If a bubble bigger than the critical size had nucleated anywhere in our past light cone, it would have engulfed us by now, and we would not find ourselves in the EW vacuum now. The (dimensionless) volume of our past light cone is about $V_4 \sim (1/m_t^4)\exp(404)$, which is nothing but our Hubble 4-volume in $1/m_t^4$ units, and we choose this unit since our starting point for the running is at the m_t scale. Thus, the total probability that we would have nucleated a bubble in our Hubble volume and tunneled into the true vacuum by now is $P_{\rm tunl} \sim (dP_{\rm tunl}/dV_4)V_4$, which gives [1]

$$P_{\rm tunl} = (h_0/m_t)^4 e^{(404 - S_B)}. \tag{30}$$

If $P_{\rm tunl} \ll 1$ for the given $V_{\rm eff}$, we deem this as an acceptable situation. In other words, if $P_{\rm tunl} \gtrsim 1$, we take this to mean that the probability that we would have tunneled into the true vacuum due to a bubble nucleating in our past light cone is essentially unity, and therefore the model that generated that $V_{\rm eff}$ we consider is disfavored. Evidently, the larger S_B is, the smaller $P_{\rm tunl}$ is, and the latter is exponentially suppressed by S_B. In the following section, we numerically solve the bounce EOM to get the bounce configuration $h_B(\rho)$, compute S_B for this h_B, and compute $P_{\rm tunl}$. We do this for the SM and some VLF extensions.

B. Tunneling probability numerical results

Here, we describe the method we use to solve the bounce EOM numerically and obtain the bounce configuration $h_B(\rho)$, the bounce action S_B, and the tunneling probability $P_{\rm tunl}$ for the SM and various VLF extensions.

The value of S_B largely depends on the behavior of $V_{\rm eff}$ at large field values h where the h^4 term dominates, which is why we included only that term in $V_{\rm eff}$. Nevertheless, for completeness, we insert an EW minimum at v by including it in $\lambda(h)$ for $h \sim v$ as follows. Keeping the h^2 term, we have for $h \sim v$ the potential $V = -(\mu_h^2/2)h^2 + (\lambda/4)h^4$, which we define to be $V_{\rm eff} = (\lambda(h)/4)h^4$ as in Eq. (3). This definition implies that we have the effective quartic coupling given by $\lambda(h) = \lambda(v)(1 - 2v^2/h^2)$ for $h \sim v$. Slightly above the scale v, we match this to the $\lambda(h)$ obtained by solving the RGE. In this way, we effectively obtain a minimum at $h = v$, while the larger field value evolution is governed by the RGE. We add a constant term to $V_{\rm eff}$ and make $V_{\rm eff}(v) = 0$.

We obtain a solution of the EOM in Eq. (28) numerically, subject to the BC $h(\rho = 0) = h_0$, $(dh/d\rho)(\rho = 0) = 0$. h_0 is unknown, and so we iteratively search for that h_0 that will lead to $h(\rho_{\rm end}) = v$ and $(dh/d\rho)(\rho_{\rm end}) = 0$. Although in theory $\rho_{\rm end} \to \infty$, in practice, it can be picked finite but large enough that the bounce has completed the transition from h_0 to v. In our numerical implementation, we work with the dimensionless quantities $\hat{\rho} \equiv \tilde{m}_t \rho$, $\hat{h} \equiv h/\tilde{m}_t$, and $\hat{V}_{\rm eff}(h) = V_{\rm eff}(h)/{\tilde{m}_t}^4$.

The friction term that goes like $1/\rho$ in Eq. (28) will be problematic numerically near $\rho \to 0$, and we therefore obtain an analytical solution in this region, valid for $\hat{\rho} \in (0, \epsilon)$ for $\epsilon \ll 1$, and match this onto a numerical solution of the EOM for $\hat{\rho} \geq \epsilon$. We now give the solution valid in $\hat{\rho} \in (0, \epsilon)$. For small $\hat{\rho}$, we expand as $(3/\hat{\rho})d\hat{h}/d\hat{\rho} \equiv s(\hat{\rho}) = s_0 + s_1\hat{\rho} + (s_2/2)\hat{\rho}^2 + \mathcal{O}(\hat{\rho}^3)$ and require all the s_i to be finite so that the friction term is finite as $\hat{\rho} \to 0$. Integrating this, we find $\hat{h}(\hat{\rho}) = \hat{h}_0 + (s_0/6)\hat{\rho}^2 + \mathcal{O}(\hat{\rho}^3)$. Differentiating the earlier equation, we have $d^2\hat{h}/d\hat{\rho}^2 = s_0 + (4s_1/3)\hat{\rho} + (5s_2/6)\hat{\rho}^2 + \mathcal{O}(\hat{\rho}^3)$. We find $\lambda(\hat{h}(\hat{\rho})) = \lambda_0 + (\beta_{\lambda 0}/\hat{h}_0)(d^2\hat{h}/d\hat{\rho}^2)_0\hat{\rho}^2/2 + \mathcal{O}(\hat{\rho}^3)$, and $\beta_\lambda(\hat{h}(\hat{\rho})) = \beta_{\lambda 0} + (\partial\beta_\lambda/\partial\hat{h})_0(d^2\hat{h}/d\hat{\rho}^2)_0\hat{\rho}^2/2 + \mathcal{O}(\hat{\rho}^3)$, where $\lambda_0 \equiv \lambda(h_0)$, $\beta_{\lambda 0} \equiv \beta_\lambda(h_0)$, $(d^2\hat{h}/d\hat{\rho}^2)_0 \equiv (d^2\hat{h}/d\hat{\rho}^2)(\hat{\rho} = 0)$, and $(\partial\beta_\lambda/\partial\hat{h})_0 \equiv (\partial\beta_\lambda/\partial\hat{h})(\hat{h} = \hat{h}_0)$. Also, $\partial\hat{V}_{\rm eff}/\partial\hat{h} = [\lambda(\hat{h}) + \beta_\lambda(\hat{h})/4]\hat{h}^3$. Substituting these into the EOM in Eq. (28), we get, by matching powers of $\hat{\rho}$, $s_0 = (\lambda_0 + \beta_{\lambda 0}/4)\hat{h}_0^3/2$, $s_1 = 0$, and $s_2 = (3/8)(d^2\hat{h}/d\hat{\rho}^2)_0[3(\lambda_0 + \beta_{\lambda 0}/4)\hat{h}_0 + (\beta_{\lambda 0}/\hat{h}_0 + (\partial\beta_\lambda/\partial\hat{h})_0/4)\hat{h}_0^3]$. This is the solution valid for $\hat{\rho} \in (0, \epsilon)$, and we get the solution at $\hat{\rho} = \epsilon$ by substituting $\hat{\rho} = \epsilon$ in this.

Taking the $\hat{h}(\epsilon)$ and $(d\hat{h}/d\hat{\rho})|_\epsilon$ obtained as above at the point ϵ as a BC, we numerically integrate the EOM in Eq. (28) for $\hat{\rho} \in (\epsilon, \hat{\rho}_{\rm end})$ and obtain $\hat{h}_B(\hat{\rho})$ over this domain. The large values of the fields and the presence of the friction term complicate the numerical implementation. A further challenge is that satisfying the required end condition requires an extremely sensitive tuning of the starting value $\hat{h}_0$. By an iterative search algorithm, we are able to obtain the bounce configuration $h_B(\hat{\rho})$ using *Mathematica*.

Piecing together the analytical solution above and the numerical solution, we obtain the bounce configuration over the complete domain $\hat{\rho} \in (0, \hat{\rho}_{\rm end})$. Following this procedure, we present below the bounce configuration, the bounce action evaluated for this bounce, and the tunneling probability for the SM and various VLF extensions.

For the SM, the $V_{\rm eff}(h \equiv \mu)$ and the bounce configuration $h_B(\rho)$ obtained numerically are shown in Fig. 5. The $V_{\rm eff}(\mu)$ is positive for smaller μ, crosses zero at about $\mu \approx 10^{10.75}$ GeV, and is negative for larger μ. The blue dot shows the starting field value (h_0) of the bounce, and the red dot shows the ending field value (v). For this bounce, we find by numerical integration of Eq. (29) that the value of the Euclidean bounce action is $S_B = 2866$ (in $\hbar = 1$ units). From this, we compute the tunneling probability into the true vacuum in our Hubble volume from Eq. (30) to be $P_{\rm tunl} \sim 10^{-1013}$, which is an incredibly small probability. This and many other comparisons we have done for the SM are in excellent agreement with the results obtained in Ref. [4].

Next, we solve the bounce EOM and compute the S_B and $P_{\rm tunl}$ for various VLF representations. We start with a (color singlet) VLL family with SM-like hypercharge assignment present, i.e., an $SU(2)$ singlet with hypercharge -1 and an $SU(2)$ doublet VLL with hypercharge $-1/2$ both present, for various common mass M_{VL} and various $\tilde{y}$.

For a VLL family with $M_{VL} = 10^3$ GeV and $\tilde{y} = 0.6$, the $V_{\rm eff}(h \equiv \mu)$, and the bounce configuration are shown in Fig. 6 (top row). The $V_{\rm eff}(\mu)$ is positive for smaller μ, crosses zero at about $\mu \approx 10^{6.5}$ GeV, and is negative for larger μ. The blue dot shows the starting field value (h_0) of the bounce, and the red dot shows the ending field value (v). For this bounce configuration, we find $S_B = 472$ and $P_{\rm tunl} \sim 10^{-6}$. This parameter-space point is thus acceptable as the tunneling probability into the true vacuum is sufficiently small for us to understand why the electroweak

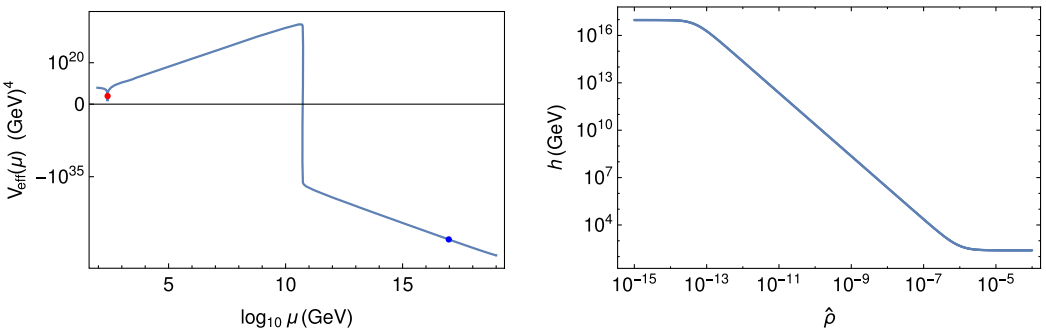

FIG. 5. For the SM, the effective potential as a function of the field value $h = \mu$ and the bounce configuration $h_B(\hat{\rho})$. The blue (red) dot shows the starting (ending) value of the bounce.

vacuum has still not tunneled away into the true vacuum within the age of the Universe. That is, for this model with VLL present, the probability of a true vacuum bubble having nucleated in our past light cone is sufficiently small, although this probability is much larger than in the SM. We see that the presence of a VLL increases the tunneling probability dramatically compared with the SM. For another example, we consider a VLL family with $M_{VL} = 10^3$ GeV

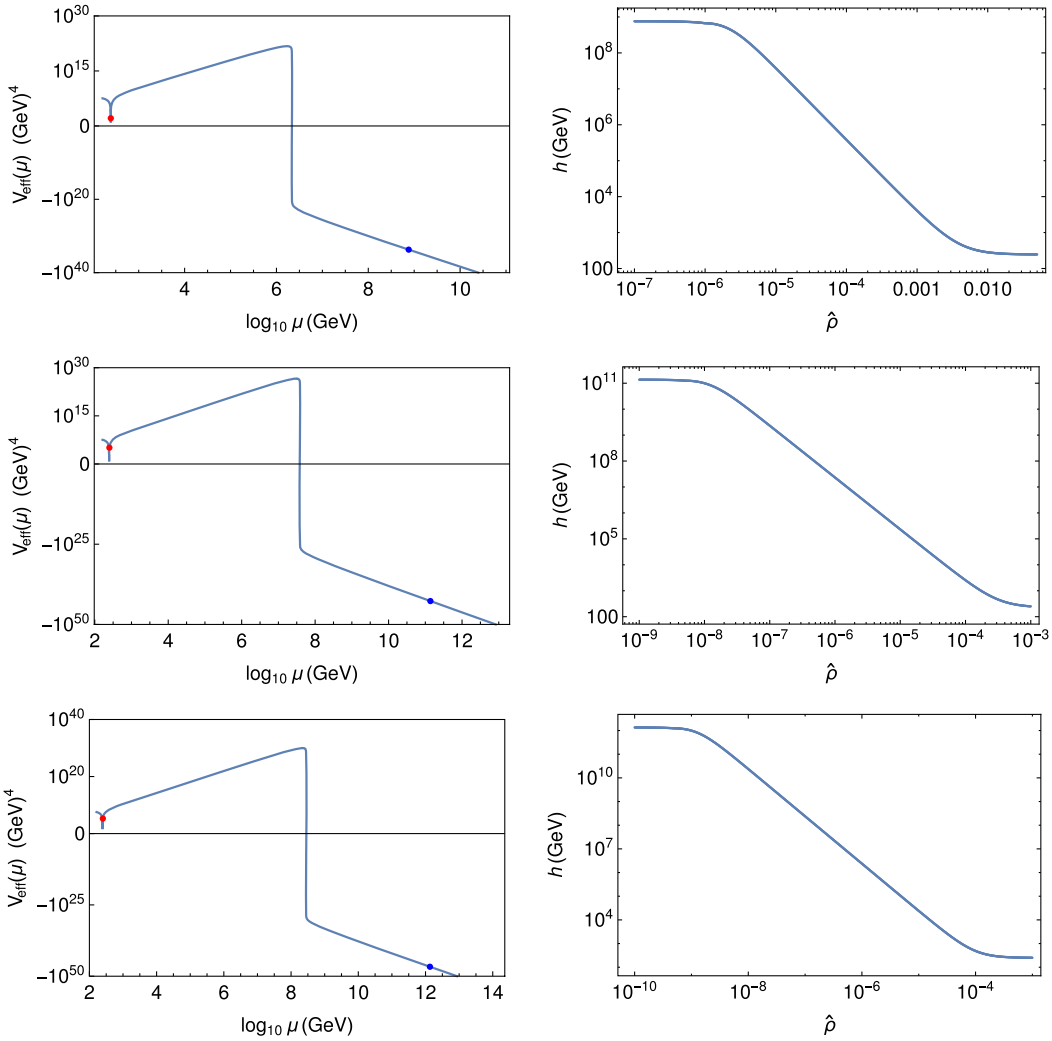

FIG. 6. For a VLL family with $M_{VL} = 10^3$ GeV and $\tilde{y} = 0.6$ (top row), $M_{VL} = 10^5$ GeV and $\tilde{y} = 0.57$ (middle row), and $M_{VL} = 10^7$ GeV and $\tilde{y} = 0.6$ (bottom row), the effective potential as a function of the field value $h = \mu$ and the bounce configuration $h_B(\hat{\rho})$. The blue (red) dot shows the starting (ending) value of the bounce.

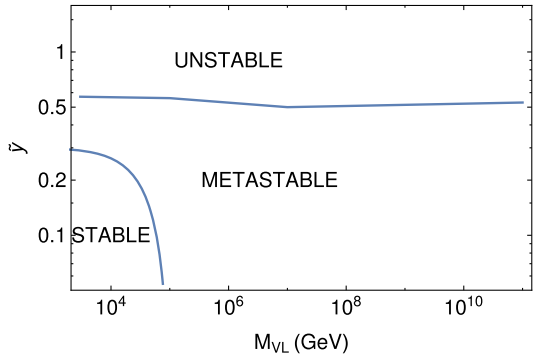

FIG. 7. With the addition of a VLQ family, the regions of stability, metastability, and instability as a function of M_{VL} (in GeV) and $\tilde{y}$.

and $\tilde{y} = 0.61$, for which we find $S_B = 422$ and $P_{\text{tunl}} \sim 10^{17}$. This large value implies that the EW vacuum could have tunneled into the true vacuum in our Hubble volume essentially with unit probability. Therefore, this parameter-space point can be considered severely disfavored. These two examples also show that P_{tunl} is extremely sensitive to $\tilde{y}$, with a small change of 0.01 in $\tilde{y}$ between the two cases resulting in a change of S_B of 50, which in turn results in a P_{tunl} 23 orders of magnitude different because of its exponential dependence on S_B. As another example, for a VLL family with $M_{VL} = 10^5$ GeV and $\tilde{y} = 0.57$, the bounce configuration is shown in Fig. 6 (middle row). For this bounce configuration, we find $S_B = 498$ and $P_{\text{tunl}} \sim 10^{-7}$, which is acceptable. For a VLL family with $M_{VL} = 10^7$ GeV and $\tilde{y} = 0.6$, the bounce configuration is shown in Fig. 6 (bottom row). For this bounce configuration, we find $S_B = 500$ and $P_{\text{tunl}} \sim 10^{-4}$, which is acceptable.

The hidden-sector Higgs-portal dark matter model of Ref. [11] essentially behaves like a VLL family considered above, for the following reason. Although in the model of Ref. [11] the VLF dark matter is a singlet and does not couple directly to the Higgs, due to the Higgs mixing with a hidden-sector scalar, a coupling with the Higgs is induced with size $\tilde{y} \equiv \kappa s_h$, where the right-hand side is in the notation of that paper and involves the parameters of that model. As can be inferred from the analysis in Ref. [11], we require $\tilde{y} \ll 1$ to keep the direct-detection rate small in order to honor experimental constraints. Thus, from the results above, we infer that EW vacuum stability constraints are not too severe in such models.

Next, we compute S_B and P_{tunl} with a color triplet VLQ family with the SM-like hypercharge assignment present, consisting of an $SU(2)$ singlet VLQ with hypercharge $2/3$ and an $SU(2)$ doublet VLQ with hypercharge $1/6$ both present, for various common mass M_{VL} and various $\tilde{y}$. With the addition of a VLQ family, in Fig. 7, we show the regions of stability, metastability, and instability as a function of M_{VL} (in giga-electron-volts) and $\tilde{y}$. In the region marked "stable," the Higgs electroweak minimum is the absolute minimum and is discussed further in Sec. IV; in the region marked "metastable," there is a lower minimum at large field values with $P_{\text{tunl}} \lesssim \mathcal{O}(1)$, and in the region marked "unstable," $P_{\text{tunl}} \gtrsim \mathcal{O}(1)$. We find that for $\tilde{y} \gtrsim 0.5$, the $P_{\text{tunl}} \gtrsim \mathcal{O}(1)$ quite independently of M_{VL}. This parameter space leads to an unstable vacuum, and we consider this region disfavored from the vacuum stability point of view.

1. Second minimum in V_{eff}

Thus far, we have investigated the situation when only the VLF is present and the effective potential has only a minimum at v and no second minimum at large field values but rather runs off in a bottomless manner. If the VLF is accompanied by other states, presumably in a UV completion that it is a part of, one can contemplate the possibility of the potential being turned around due to the contributions of the extra states and the appearance of a second minimum at large field values. We encode this possibility by adding a second minimum in the effective potential as shown in Fig. 8 for the case of a VLQ family with $M_{VL} = 3 \times 10^3$ GeV and $\tilde{y} = 0.75$. The $V_{\text{eff}}(h \equiv \mu)$ and the bounce configuration for this modified potential are shown in Fig. 8. The $V_{\text{eff}}(\mu)$ is positive for smaller

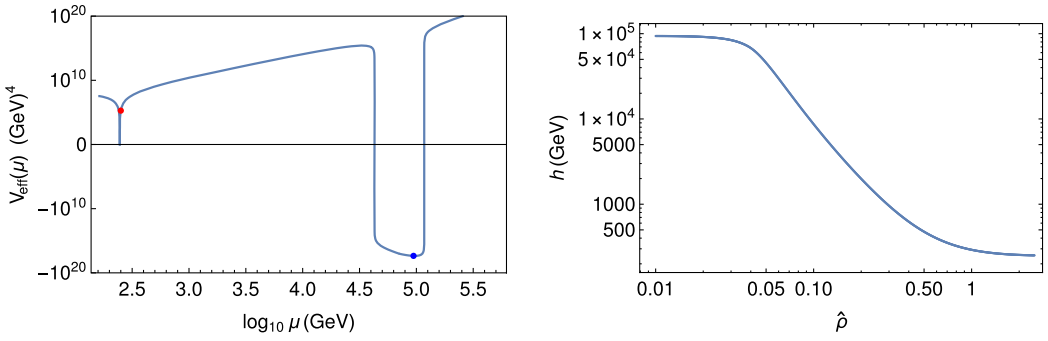

FIG. 8. For a VLQ family with $M_{VL} = 3 \times 10^3$ GeV and $\tilde{y} = 0.75$, with a second minimum in the effective potential, the effective potential as a function of the field value $h = \mu$, and the bounce configuration $h_B(\hat{\rho})$. The blue (red) dot shows the starting (ending) value of the bounce.

μ, crosses zero at about $\mu \approx 10^{4.65}$ GeV and becomes negative, obtains a minimum at about $\mu \approx 10^5$ GeV, and crosses zero again and becomes positive for larger μ. The blue dot shows the starting field value (h_0) of the bounce, and the red dot shows the ending field value (v). For this bounce configuration, we find $S_B = 3071$ and $P_{\rm tunl} \sim 10^{-1150}$, which is an incredibly tiny tunneling probability and very comfortably acceptable.

The reason why this parameter-space point, which was excluded if no second minimum was present as found earlier, is now allowed if a second minimum present is as follows. In the bounce configuration for this situation, the field value starts close to the second minimum and stays there for a substantial amount of time (i.e., ρ) near the minimum since $d\phi/d\rho$ is small there, and as a result, the friction term starts reducing in significance due to its $1/\rho$ behavior. Since the friction term becomes small, the field value can overcome the barrier and reach v. (It can even overshoot v, leading to an imaginary solution if the initial value of the field is chosen too big.) Therefore, the starting field value is much lower compared to the earlier case without the second minimum, and we find that the resulting S_B is much larger and $P_{\rm tunl}$ is much smaller, now allowing a parameter-space point that was excluded earlier.

IV. ABSOLUTE STABILITY OF THE EW VACUUM

We have seen that the EW vacuum is metastable in the SM as there is a deeper minimum below the EW vacuum albeit shielded by a potential barrier, and due to the tunneling probability being incredibly small, the lifetime of the metastable vacuum is extremely large compared to the age of the Universe. In Sec. III, we added VLFs and analyzed regions of $\tilde{y}$ and M_{VL} parameter space for which there again is a deeper minimum making the EW vacuum metastable. We computed the tunneling probability and found that in some regions of parameter space, $P_{\rm tunl}$ is acceptably small while in others it is unacceptably large. In this section, we highlight VLF cases where the addition of VLFs makes the EW vacuum the global minimum, rendering it absolutely stable.

Consider first adding some number of either $SU(3)$ singlet VLQs or doublet VLQs, but not both. For instance, we showed in Sec. II C, Fig. 1, that when three, four, or five $SU(2)$ singlet VLQs all with 3 TeV mass are added, $\lambda(h)$ never goes negative, implying that the EW minimum is the global minimum and absolutely stable, unlike the SM situation. The reason for this behavior is explained in detail in Sec. II C. As we show in Fig. 2, the same conclusion holds also when we add one to four $SU(2)$ doublet VLQs with a 3 TeV mass or one doublet with mass less than about 10^5 GeV. When both singlet and doublet VLFs are present, i.e., when a VLF family is added, the situation changes since a Yukawa coupling ($\tilde{y}$) with the Higgs can be written down. Nevertheless, when $\tilde{y}$ is small, the behavior is similar to the above two cases. For a VLQ family with one singlet and one doublet VLQ added, as can be seen in Fig. 4, for a small $\tilde{y} = 0.1$ and for $M_{VL} \lesssim 10^5$ GeV, the EW minimum becomes absolutely stable. Thus, as we see in these examples, the presence of $SU(2)$ singlet VLQs, doublet VLQs, or a full family with a small enough $\tilde{y}$ allows the intriguing possibility that the EW vacuum is rendered absolutely stable.

For example, the hidden-sector dark matter model in Ref. [47] contains a singlet VLQ mediating loop-level couplings between the hidden-sector dark matter and the SM. Such models can also be written down with a doublet VLQ. For proper choices of the number of VLQs and masses, it is interesting that the Higgs vacuum could be absolutely stable in such models, unlike in the SM in which it is metastable.

V. COMPARISON WITH THE ANALYTICAL APPROXIMATION OF S_B

Here, we compare our numerical results for S_B obtained in Sec. III B with an analytical approximation developed in Refs. [48,49], which is

$$S_B^{\rm approx} = \frac{8\pi^2}{3(-\lambda(t))}, \tag{31}$$

where t is a typical scale at which the bounce makes the transition from large field values to v. This approximation can yield a reasonably good estimate of S_B when the bounce transition happens at a fairly constant value of $\lambda(t)$, i.e., when h_0 is close to where $\beta_\lambda(h_0) \approx 0$. Furthermore, when S_B is so large that errors due to the transition not happening at a constant $\lambda(t)$ are small compared to S_B, this approximation yields a good enough estimate. When these conditions are not realized, one has to be cautious in using the expression in Eq. (31). We elaborate on this statement below with many examples.

In Fig. 9, in the left column, we show $\beta_\lambda(\mu)$ vs μ where $\mu \equiv h(\rho)$. In the right column, we show the (absolute value of the) integrand of Eq. (29), made dimensionless by multiplying the integrand by $1/m_t^4$ and denoted as $|\hat{I}(\hat{\rho})|$ vs $\lambda(h(\rho))$, with ρ being the parameter (not shown). As shown in the topmost row in Fig. 9, for the SM, it is evident that most of the contribution to the integral comes from when λ takes a specific value. For the SM, we can compare the S_B computed numerically in Sec. III B, which is 2866, with the S_B from the approximation in Eq. (31) with the t taken to be at the scale at which $\beta_\lambda = 0$ where $\lambda = -0.009$, which gives $S_B^{\rm approx} = 2848$. This is in excellent agreement with our numerical computation of S_B, and as discussed earlier, this is because $\beta_\lambda = 0$ does get satisfied for the SM, presenting a natural choice for t. That this approximation works is also borne out by the plot showing $|\hat{I}(\hat{\rho})|$ for the SM, where most of the

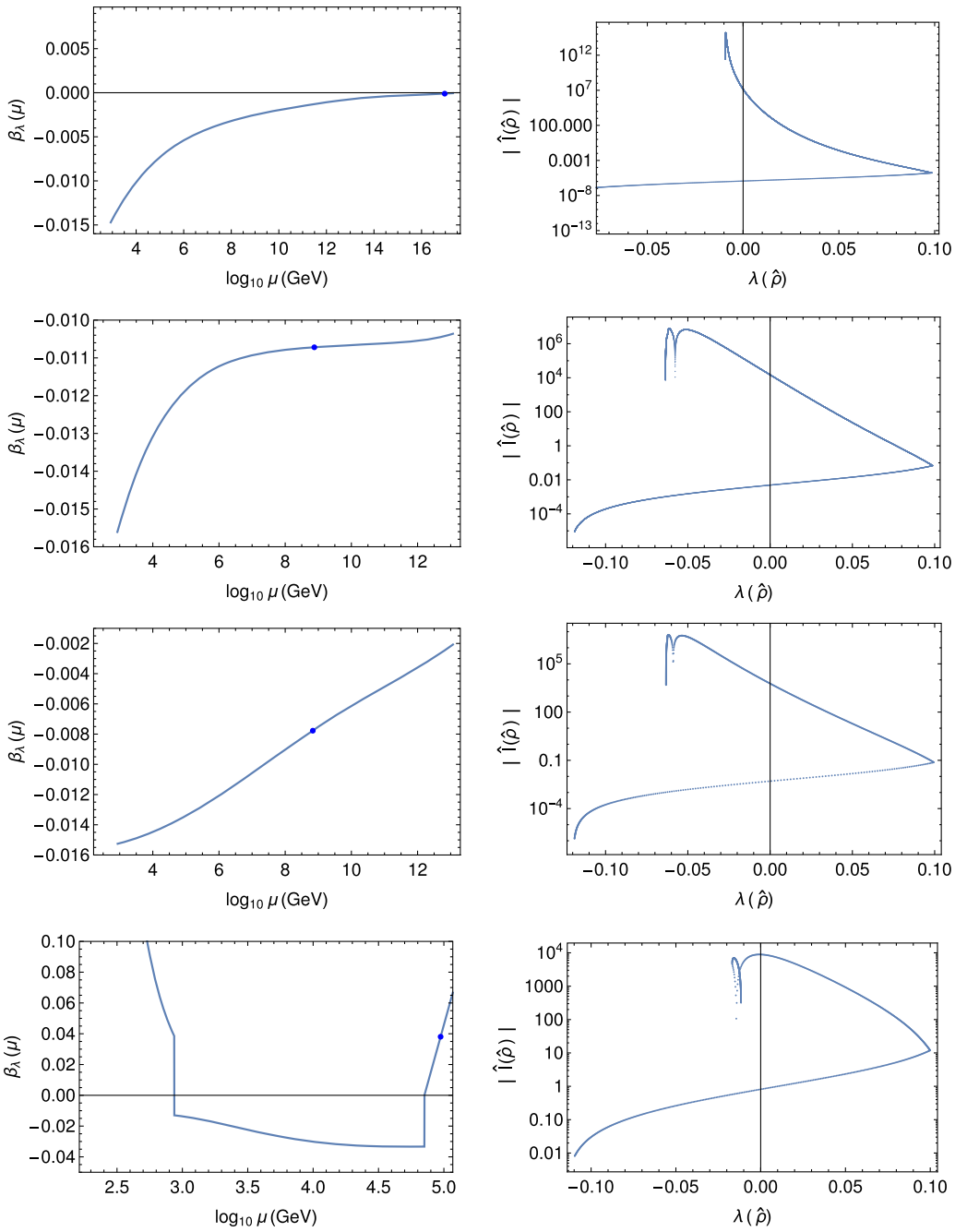

FIG. 9. The $\beta_\lambda(\mu)$ as a function of the field value $h(\rho) = \mu$ (left column) and the integrand of the bounce action integral Eq. (29) vs $\lambda(h(\rho))$ (right column), for the SM (cf. Fig. 5) (top row) and the remaining for the different cases with a VLF family as follows: a VLL family with $M_{VL} = 10^3$ GeV and $\tilde{y} = 0.6$ (cf. Fig. 6) (top row), a VLQ family with $M_{VL} = 3 \times 10^3$ GeV and $\tilde{y} = 0.57$, and a VLQ family with $M_{VL} = 3 \times 10^3$ GeV and $\tilde{y} = 0.75$ with a second minimum (cf. Fig. 8). The blue dot shows the starting value h_0 for the bounce configuration.

contribution to the S_B integral is indeed coming for $\lambda = -0.009$, where the bounce spends most of its time ($\hat{\rho}$). Indeed, Eq. (31) was put forth for the SM, where it can be safely applied.

As we see from the last three rows in Fig. 9, with VLF present, β_λ is not close to zero anywhere, and thus there is no clear choice of t that is suggested. In such a situation, we cannot use Eq. (31) but have to compute S_B numerically. Indeed, as the $|\hat{I}(\hat{\rho})|$ for these cases show, the integral gets its contributions for a range of λ. These show the inadequacy of the approximate formula and that a numerical evaluation is necessary. We have therefore computed the bounce EOM numerically and the bounce action for it, from which we computed the tunneling probability.

VI. CONCLUSIONS

We study the stability of the electroweak vacuum in the presence of new vectorlike fermions. We work with the one-loop renormalization group improved Higgs effective potential, identifying the Higgs field value $h \equiv \mu$. We first review the computation of the beta-functions in the SM, paying particular attention to the SM fermion contributions. We use dimensional regularization for our computation. We then derive the VLF contributions to the one-loop beta-functions, which can be applied to various $SU(3)$ and $SU(2)$ representations, namely VLQs and VLLs. We apply this to a few example cases with singlet VLFs, doublet VLFs, and a family consisting of one doublet VLF and one singlet VLF coupled to the Higgs via the Yukawa coupling $\tilde{y}$. We numerically run the RGE to determine the scale at which $\lambda(\mu)$ becomes zero and goes negative.

The Higgs effective quartic coupling $\lambda(\mu)$ becoming negative signals that the EW vacuum is a false vacuum and is unstable and can tunnel away quantum mechanically via barrier penetration to (large) field values that have a lower effective potential. We compute the probability P_{tunl} that the EW vacuum would have tunneled away by a true-vacuum bubble nucleating in our Hubble 4-volume. Computing P_{tunl} requires computing the bounce configuration in Euclidean space-time and the value of the Euclidean action S_B for the bounce configuration. We solve the bounce configuration EOM numerically and compute S_B for it.

We compare our numerical evaluation with the approximation commonly used for S_B, which is written in terms of λ at a single scale where $\beta_\lambda(\mu)$ is approximately zero. This is because the bounce transition is mostly completed when $\lambda(\mu)$ has this value. For the SM, there is such a scale which is about 10^{16} GeV, and we verify by comparing with our numerical evaluation that the approximation is perfectly adequate. When VLFs are present, there is no scale at which $\beta_\lambda(\mu)$ is close to zero, and so the approximation cannot be applied. A numerical evaluation is then required, which we resort to.

We take example cases where a single VLL or VLQ family is added and show the bounce transition, compute S_B for it, and obtain P_{tunl}. We find that P_{tunl} is extremely sensitive to $\tilde{y}$ as it exponentially depends on S_B. Interestingly, we find that for some VLF representations and parameters, adding only singlet VLFs, a doublet VLFs, or a full family with a small enough $\tilde{y}$, λ stays positive to arbitrarily large scales; i.e., the EW vacuum is rendered absolutely stable, unlike in the SM in which it is metastable. For other parameters, adding VLFs still keeps the EW vacuum metastable, either with a larger P_{tunl} than in the SM or a smaller P_{tunl}.

In summary, our work here helps us get an idea of what the impact of VLFs is on the stability of the Higgs electroweak vacuum.

ACKNOWLEDGMENTS

We thank Romesh Kaul for valuable discussions.

APPENDIX A: SM β-FUNCTIONS (FERMION CONTRIBUTIONS)

Here, we review the calculation of the fermion contributions to the one-loop β-functions in the SM so that we can extend this to include VLF contributions in the next section. Since we are interested in field values h much larger than the particle masses, we neglect the particle masses.

We expand the SM Lagrangian density shown in Eq. (5) by writing the Higgs doublet as $H = (1/\sqrt{2})((\phi^1 + i\phi^2)(v + h + i\phi^3))^T$, where $v \approx 246$ GeV is the EW VEV, h is the physical Higgs boson, and ϕ^i are the Goldstone bosons. The Lagrangian density in terms of the bare fields $\{\tilde{h}, t_0\}$ and bare coupling y_0 is

$$\mathcal{L} \supset \bar{t}_0 i\not{D} t_0 + \frac{1}{2}[(D_\mu \tilde{h})^2 + (D_\mu \phi_0^i)^2] - \left[\frac{y_0}{\sqrt{2}}(\bar{t}_0(\tilde{h} + i\gamma^5\phi_0^3)t_0 - \bar{t}_0(\phi_0^1 + i\phi_0^2)P_L b_0) + \text{H.c.}\right], \tag{A1}$$

where for notational brevity we denote y_t just as y and the covariant derivatives are in the usual notation. In terms of the renormalized fields and counterterms, we have for the $\{t, h\}$ sector

$$\mathcal{L} \supset \bar{t} i\not{D} t + \frac{1}{2}(D_\mu h)^2 - \left(\frac{y}{\sqrt{2}} h\bar{t}t + \text{H.c.}\right) + \frac{1}{2}(Z_h - 1)(D_\mu h)^2 + (Z_{t_{L,R}} - 1)\bar{t}_{L,R} i\not{D} t_{L,R} - \left[\frac{y}{\sqrt{2}}\left(Z_y\sqrt{Z_h Z_{t_L} Z_{t_R}} - 1\right) h\bar{t}t + \text{H.c.}\right], \tag{A2}$$

where the renormalized fields h, t are defined by $\tilde{h} = \sqrt{Z_h}h$, $t_{0L,R} = \sqrt{Z_{t_{L,R}}}t_{L,R}$ and the renormalized Yukawa coupling y is defined by $y_0 = Z_y y$. Expanding as a perturbation series in y, we define a's to leading order as $(Z_h - 1) \equiv a_h y^2/2$, $(Z_{t_{L,R}} - 1) \equiv a_{t_{L,R}} y^2/2$, $(Z_y - 1) \equiv a_y y^2/2$, and we also define $(\hat{Z}_y - 1) \equiv (Z_y\sqrt{Z_h Z_{t_L} Z_{t_R}} - 1) = (a_y + a_h/2 + a_{t_L}/2 + a_{t_R}/2)y^2/2 \equiv \hat{a}_y y^2/2$. Similarly, the renormalized Lagrangian density for the Goldstone fields can be written down.

The Feynman vertices in momentum space are as follows:

(i) propagator $(t_{L,R}t_{L,R})(p)$ is $i\not{p}/(p^2 + i\epsilon)$ with the counterterm $ia_{t_{L,R}}\not{p}y^2/2$

(ii) propagator $(hh)(p)$ is $i/(p^2 + i\epsilon)$ with the counterterm $ia_h p^2 y^2/2$

(iii) Yukawa coupling $ht\bar{t}$ is $-iy/\sqrt{2}$ with the counterterm $-i\hat{a}_y y^3/(2\sqrt{2})$

(iv) for the Goldstone bosons, the Yukawa coupling $\phi^3 t\bar{t}$ is $-y\gamma^5/\sqrt{2}$ with the counterterm $\hat{a}_y y^3\gamma^5/(2\sqrt{2})$, and $\phi^{1,2}b\bar{t}$ is $iyP_L(1,i)/\sqrt{2}$ with the counterterm $-i\hat{a}_y y^3 P_L(1,i)/(2\sqrt{2})$.

We give next the one-loop corrections involving the t, which we compute using dimensional regularization. We present only the SMF t contributions, since our goal is to use these to derive the VLF contributions to the β-functions later.

The one-loop correction to the Higgs two-point function (wave function renormalization of the h) due to the fermion is $i\Sigma_h(p_h) = i(N_c y^2/(8\pi^2))p_h^2(1/\epsilon - \ln p_h - i\pi/2 + \ln\sqrt{4\pi} - \gamma/2 + \mathcal{O}(\epsilon))$, after including a factor of (-1) for the fermion loop, where $\gamma \approx 0.5772$ is the Euler-Mascheroni constant. To cancel this divergence, we fix the counterterm from the condition $i\Sigma_h(p_0) + ia_h p_0^2 y^2/2 = 0$ at the subtraction scale p_0. As mentioned above, since our goal is to derive the t contributions to the β-functions, we show only the y dependent terms in the counterterms, and we omit other terms. This yields $a_h = -N_c/(4\pi^2)(1/\epsilon - \ln p_0 - i\pi/2 + \cdots)$, and we have

$$i\Sigma_h(p_h) + ia_h\frac{y^2}{2}p_h^2 = -i\frac{N_c y^2}{8\pi^2}p_h^2\ln\left(\frac{p_h}{p_0}\right). \tag{A3}$$

The one-loop correction to the fermion two-point function (wave function renormalization of the $t_{L,R}$) proportional to y is $i\Sigma_{t_{L,R}}(p_t) = iy^2/(32\pi^2)\not{p}_t(1/\epsilon - \ln p_t/2 + \ln\sqrt{4\pi} - \gamma/2 + \mathcal{O}(\epsilon))$, and to cancel the divergence, we fix the counterterm from the condition $i\Sigma_t(p_0) + ia_t\not{p}_0 y^2/2 = 0$, which yields $a_{t_{L,R}} = -1/(16\pi^2)(1/\epsilon - \ln p_0/2 + \ln\sqrt{4\pi} - \gamma/2)$, and we have $i\Sigma_{t_{L,R}}(p_t) + ia_{t_{L,R}}\not{p}_t y^2/2 = -iy^2/(32\pi^2)\not{p}_t \ln p_t/p_0$. The vertex one-loop correction proportional to y is

$$iV(p_h) = iy^3/(16\sqrt{2}\pi^2)(1/\epsilon - \ln p_h/2 + \ln\sqrt{4\pi} - \gamma/2 + 1/2 + \mathcal{O}(\epsilon)),$$

where we take the Higgs momentum as p_h and the fermion momenta as $-p_h/2$ and $p_h/2$. To cancel the divergence, we fix the vertex counterterm from the condition $iV(p_0) - i\hat{a}_y = 0$, which yields $iV(p_h) - i\hat{a}_y y^3/(2\sqrt{2}) = -iy^3/(16\sqrt{2}\pi^2)\ln p_h/p_0$, and we have

$$a_y = (2N_c+3)/(16\pi^2)(1/\epsilon - \ln p_0/2 + \ln\sqrt{4\pi} - \gamma/2 + 1 - \ln 2/(2N_c+3)).$$

We discuss next the Goldstone boson contributions proportional to y. Starting with the self-energy corrections, we have the ϕ^3 contribution to $\Sigma_{t_{L,R}}$ is equal to the h contribution, the ϕ^1 and ϕ^2 contributions to Σ_{t_R} are equal to the h contribution, and, the ϕ^1 and ϕ^2 contributions to Σ_{t_L} are proportional to y_b which we drop and take to be zero. Turning next to the vertex corrections, we have the ϕ^3 contribution to the $ht_L\bar{t}_R$ vertex (V_{LR}) is negative of the h contribution to this vertex, the ϕ^3 contribution to the $ht_R\bar{t}_L$ vertex (V_{RL}) is again negative of the h contribution to this vertex, and, the $\phi^{1,2}$ contribution to $V_{LR,RL}$ is proportional to y_b and hence we take it to be zero.

One way to extract the β-function is from the divergent part of the bare coupling.[3] From the contributions computed above, we find the contributions proportional to y to be $y_0 \supset y + (y^3/(16\pi^2))((3+2N_c)/2)(1/\epsilon)$, from which we obtain the fermionic contribution to β_y as

$$\beta_y \supset \frac{y^3}{16\pi^2}\left[\frac{(3+2N_c)}{2}\right], \tag{A4}$$

after including the $t, h, \phi^{1,2,3}$ contributions. This is in agreement with the results in Refs. [4,50], for example. Interestingly, the $\phi^{1,2,3}$ contribute zero after including all their contributions.

The yg_3^2 and yg_2^2 contributions to β_y can be written as [4]

$$\beta_y \supset \frac{y}{16\pi^2}\left(-8g_3^2 - \frac{9}{4}g_2^2\right), \tag{A5}$$

which are included in Eq. (8). To derive the yg_1^2 contribution, we start by extracting the relevant Feynman rules for the hypercharge gauge boson B_μ interactions. With all momenta going into the vertex, with $Y_{L,R}$ being the hypercharges of $\psi_{L,R}$ and $Y_H = 1/2$ being the hypercharge of the Higgs doublet, we have the Feynman rules:

$$\begin{aligned}\phi^3(p_3)h(p_h)B_\mu &: -g'Y_H(p_3^\mu - p_h^\mu);\\ hhB_\mu B_\nu &: 2ig'^2Y_H^2 g_{\mu\nu};\\ hB_\mu B_\nu &: 2ig'^2Y_H^2 v g_{\mu\nu};\\ \psi_{L,R}\bar{\psi}_{L,R}B_\mu &: ig'Y_{L,R}\gamma^\mu.\end{aligned}$$

Computing the B_μ contribution at one-loop order in the 'tHooft-Feynman $\xi = 1$ gauge, we obtain the following

[3]We briefly summarize here the method to obtain the β-function from the bare coupling, following 'tHooft's method as described in Ref. [41]. With κ_0 the bare coupling, we write in $d = 4 - \epsilon$ dimensions, $\kappa_0\mu^{-\Delta(d)} = \kappa(\mu,d) - b(\kappa(\mu,d))/\epsilon$, $\Delta(d) \equiv \Delta - \rho\epsilon$, κ_0 being μ independent, and $\kappa(\mu,d)$ is the renormalized coupling. Then, we write $d\kappa(\mu,d)/d\ln\mu \equiv \beta_\kappa - \alpha_\kappa\epsilon$ with β_κ being the β-function, and by matching powers of ϵ, we obtain $\beta_\kappa = -\Delta\kappa - \rho b + \rho\kappa\partial b/\partial\kappa$. We generalize this to a system of many couplings κ_i by writing $\kappa_{0i}\mu^{-\Delta_i(d)} = \kappa_i(\mu,d) - \sum_j b_{ij}(\kappa(\mu,d))/\epsilon$ with $\Delta_i(d) \equiv \Delta_i - \rho_i\epsilon$. Then, the β-functions are $\beta_{\kappa_i} = -\Delta_i\kappa_i - \sum_j[\rho_i b_{ij} - (\partial b_{ij}/\partial\kappa_j)\rho_j\kappa_j]$. For the couplings encountered here, we have $\Delta_y = 0, \rho_y = -1/2$; $\Delta_\lambda = 0, \rho_\lambda = -1$; and $\Delta_{g_a} = 0$, $\rho_{g_a} = -1/2$ (for $a = \{1,2,3\}$).

divergent pieces: the $\psi_R\bar{\psi}_L h$ vertex correction due to B_μ exchange gives $iV^{(B_\mu)} \supset -i8Y_L Y_R y g'^2/(\sqrt{2}16\pi^2\epsilon)$; the Higgs two-point function correction due to $\phi^3 - B_\mu$ exchange gives $i\Sigma_h^{(B_\mu)} \supset -i4g'^2 Y_H^2 p_h^2/(16\pi^2\epsilon)$; and the fermion two-point function corrections due to B_μ exchange gives $i\Sigma^{(B_\mu)}_{\psi_L,\psi_R} \supset i2g'^2 Y_{L,R}^2 \not{p}/(16\pi^2\epsilon)$. We include in the counterterms a piece to cancel these divergences at the subtraction scale p_0, i.e., $i(Z_h-1)p_0^2/2 \supset -i\Sigma_h^{(B_\mu)}(p_0)$, $i(Z_{\psi_L,\psi_R}-1)\not{p}_0 \supset -i\Sigma^{(B_\mu)}_{\psi_L,\psi_R}(p_0)$, and $i(y/\sqrt{2})(\hat{Z}_y - 1) \supset iV^{(B_\mu)}$. From these, we determine $(Z_y - 1) = -g'^2(8Y_L Y_R + 4Y_H^2 - Y_L^2 - Y_R^2)/(16\pi^2\epsilon)$. Thus, since the bare coupling is $y_0 = Z_y y$, we get the contribution

$$\beta_y \supset \frac{-yg'^2}{16\pi^2}(8Y_L Y_R + 4Y_H^2 - Y_L^2 - Y_R^2) = \frac{y}{16\pi^2}\left[-\frac{9}{5}g_1^2(Y_H^2 + 2Y_L Y_R)\right], \tag{A6}$$

where we make use of $Y_H = Y_R - Y_L$ required for $U(1)_Y$ invariance of the Yukawa term in the Lagrangian, and $g' = \sqrt{3/5}g_1$. For the top, using $Y_L = 1/6$, $Y_R = 2/3$, we obtain the contribution shown in the last term of Eq. (8).

We compute the fermion loop contribution to the Higgs four-point vertex that is proportional to y, from which we can write the bare coupling as $\lambda_0 \supset \lambda - N_c y^4/(8\pi^2)(1/\epsilon + \text{finite})$. From this, we infer that this contribution leads to

$$\beta_\lambda \supset \frac{1}{16\pi^2}[-2N_c y^4]. \tag{A7}$$

Writing the Higgs four-point vertex as $i\lambda_{\text{eff}}$, the contribution to its evolution, i.e., β_λ, due to the fermion loop in the h-leg is just four times $\sqrt{\Sigma_h}$. Thus, for this contribution, we have $i\lambda_{\text{eff}} \supset (-i\lambda)(i/p^2)(4 \times i\Sigma_\phi/2)$, and from Eq. (A3), we have $\lambda(\mu) = \lambda(M) + N_c\lambda y^2/(4\pi^2)\ln(\mu/M) + \ldots$, where μ is the renormalization scale and M is a subtraction scale. From this, and since $\beta_\lambda = d\lambda(\mu)/d\ln\mu$, we have

$$\beta_\lambda \supset \frac{1}{16\pi^2}[4N_c y^2\lambda]. \tag{A8}$$

We turn next to the β-functions of the gauge couplings $g_a = \{g_3, g_2, g_1\}$, focusing on the SM fermion contribution. We recall the definition $\beta_a = g_a^3 b_a/(16\pi^2)$. For β_{g_3}, we have the well-known result (see, for example, Ref. [41])

$$\beta_{g_3} = \frac{g_3^3}{16\pi^2}\left(-\frac{11}{3}N_c + \frac{2}{3}n_3\right), \tag{A9}$$

where the second term is due to fermions, with n_3 as the number of colored fermions in the fundamental representation of $SU(3)$. Note that the top quark is vectorlike with respect to the $SU(3)$. In the SM, at large μ, we have $n_3 = 6$ for three generations of quarks, which implies $b_3 = -7$. Similarly, for β_{g_2}, we have

$$\beta_{g_2} = \frac{g_2^3}{16\pi^2}\left(-\frac{11}{3}(2) + \frac{1}{2}\times\frac{2}{3}n_2 + \frac{1}{6}\right), \tag{A10}$$

where we have taken $N = 2$ for $SU(2)$ in the first term, the second term is the fermion $SU(2)$ doublet contribution with n_2 being the number of doublet fermions, and the last term is the Higgs doublet contribution. Since the SM fermions are chiral under $SU(2)$ with only the L chirality contributing, we include an extra factor of $1/2$ in the second term (since we are neglecting the effects of masses). Thus, in the SM, at large μ, $n_2 = (3N_c + 3)$ for the three generations of quark and lepton doublets, which yields $b_2 = -19/6$. Lastly, for β_{g_1}, we have

$$\beta_{g_1} = \frac{g_1^3}{16\pi^2}\left(\frac{2}{5}\sum_f Y_f^2 + \frac{1}{5}\sum_\phi Y_\phi^2\right), \tag{A11}$$

where the sum in the first term is over all fermions f with hypercharge Y_f and the sum in the second term is over all complex scalars ϕ with hypercharge Y_ϕ. We recall that we use $SU(5)$ normalization for g_1, i.e., the SM hypercharge gauge coupling g' is related to g_1 by $g_1 = \sqrt{5/3}g'$. Thus, in the SM, at large μ, for three generations, $\sum_f Y_f^2 = 3 \times (10/3) = 10$, and for one Higgs doublet containing two complex fields with $Y_H = 1/2$, $\sum_\phi Y_\phi^2 = 2(1/2)^2 = 1/2$, we get $b_1 = 41/10$. This agrees with, for example, Ref. [51].

We complete our derivation of the SM fermion contributions to the one-loop β-functions. After adding the other contributions, the complete one-loop β-functions are as given in Eqs. (7)–(9).

APPENDIX B: VLF CONTRIBUTIONS TO THE RGE

Here, we extend the β-functions derived in Sec. II A and Appendix A to include VLF contributions, which we denote as $\beta_\kappa^{\text{VLF}}$.

We first derive the $\beta_{g_a}^{\text{VLF}}$. The $\beta_{g_3}^{\text{VLF}}$ is gotten easily from Eq. (A9). Since the SM quark is vectorlike with respect to $SU(3)$, we have an identical contribution for a VLQ, and we obtain the result shown in Eq. (15). For obtaining $\beta_{g_2}^{\text{VLF}}$, we note that this is similar to the $SU(3)$ contribution, owing to the fact that for a VLF, $SU(2)$ is also vectorlike just as the SMF was for $SU(3)$. Thus, taking twice the second term in Eq. (A10) will give us $\beta_{g_2}^{\text{VLF}}$ as given in Eq. (16). Since for a VLF both L and R chiralities contribute, we take twice the first term in Eq. (A11) to obtain $\beta_{g_1}^{\text{VLF}}$ as given in Eq. (17); the $2n_2$ is just the number of fermions in n_2 doublets having hypercharge Y_χ.

Next, we derive the contributions present only when a full family is added, i.e., when the $\tilde{y}$ operator of Eq. (13) can be written down.

Let us recall that the SM top (and bottom) sector has the following Feynman rules for the couplings with the Higgs-doublet fields $\{h, \phi^{1,2,3}\}$ [all vertices have an overall $(-iy_t/\sqrt{2})$] written in terms of the Dirac spinors $t = (t_L t_R)^T$ and $b = (b_L b_R)^T$:

$$\{h, \phi^3\} t\bar{t}\colon \{1, -i\gamma^5\} \quad \text{and} \quad \{\phi^1, \phi^2\} b\bar{t}\colon \{-P_L, -iP_L\}.$$

Now, when a full VLF family is present, we have the $SU(2)$ doublet VLF $\chi = (\chi_1 \chi_2)^T$ and a singlet ξ. We can assemble the following Dirac spinors: $\psi_1 = (\chi_{1L} \xi_R)^T$, $\psi_2 = (\xi_L \chi_{1R})^T$, $\xi = (\xi_L \xi_R)^T$, and $\chi_2 = (\xi_{2L} \xi_{2R})^T$. Using these, we can write the Feynman rules with the Higgs-doublet fields $\{h, \phi^{1,2,3}\}$ as follows [all vertices have an overall $(-i\tilde{y}/\sqrt{2})$]:

$$\{h, \phi^3\} \psi_1 \bar{\psi}_1\colon \{1, -i\gamma^5\} \quad \text{and}$$
$$\{\phi^1, \phi^2\} \chi_2 \bar{\psi}_1\colon \{-P_L, -iP_L\},$$

$$\{h, \phi^3\} \psi_2 \bar{\psi}_2\colon \{1, i\gamma^5\} \quad \text{and}$$
$$\{\phi^1, \phi^2\} \chi_2 \bar{\psi}_2\colon \{-P_R, -iP_R\}.$$

We write it this way to bring forth the analogy between the SMF and VLF, with the realization that for the VLF, we have two Dirac sets that each have a similarity with the SM couplings. The first Dirac fermion ψ_1 has identical couplings, while the second Dirac fermion ψ_2 has couplings that is similar but not identical, with a change $i \to -i$ in the ϕ^3 couplings and $P_L \to P_R$ in the $\phi^{1,2}$ couplings. We observe that all the diagrams that contribute to the β-functions are immune to both of these changes, and therefore each of them gives the same SM contribution as for the t quark. Furthermore, the Goldstone bosons with each Dirac fermion contributes zero to the β-function as in the SM. Thus, to obtain the VLF contributions to $\beta_\lambda^{\rm VLF}$, we just multiply the SM contribution after combining Eqs. (A7) and (A8) by a factor of 2 and obtain Eq. (18). Next, the VLF contribution to β_{y_t} is due to only the wave function renormalization contribution to h, i.e., Σ_h, and this contribution can be gotten from the second term in Eq. (A4) but multiplied by 2 since there are two VLF Dirac sets as argued above and changing the coupling to $y_t \tilde{y}^2$ instead of y_t^3, which then gives us the $\beta_{y_t}^{\rm VLF}$ in Eq. (19). Next, consider the evolution of either the $h\psi_1\bar{\psi}_1$ coupling or the $h\psi_2\bar{\psi}_2$ coupling, either of which is $\tilde{y}$. The VLF contribution to $\beta_{\tilde{y}}$ is due to these three contributions: (i) the vertex contribution proportional to $3\tilde{y}^3$ as in the first term in Eq. (A4); (ii) the VLF contributions in Σ_h, which yields twice the second term in Eq. (A4) proportional to $2 \times 2N_c' \tilde{y}^3$ since each of the ψ_1 and ψ_2 contribute as in the SM; and (iii) the top-quark contribution in Σ_h, which yields $2N_c y_t^2 \tilde{y}$ as in the second term in Eq. (A4). Adding these three contributions then gives the first part of $\beta_{\tilde{y}}$ in Eq. (20). We write the $\tilde{y} g_a^2$ contributions to $\beta_{\tilde{y}}$ following Eqs. (A5) and (A6), which gives the last part in Eq. (20). We thus complete the derivation of the VLF contributions to the β-functions given in Eqs. (15)–(20).

[1] M. Sher, Phys. Rep. **179**, 273 (1989).
[2] F. Bezrukov, M. Y. Kalmykov, B. A. Kniehl, and M. Shaposhnikov, J. High Energy Phys. 10 (2012) 140.
[3] G. Degrassi, S. Di Vita, J. Elias-Miro, J. R. Espinosa, G. F. Giudice, G. Isidori, and A. Strumia, J. High Energy Phys. 08 (2012) 098.
[4] D. Buttazzo, G. Degrassi, P. P. Giardino, G. F. Giudice, F. Sala, A. Salvio, and A. Strumia, J. High Energy Phys. 12 (2013) 089.
[5] F. Bezrukov and M. Shaposhnikov, Zh. Eksp. Teor. Fiz. **147**, 389 (2015) [J. Exp. Theor. Phys. **120**, 335 (2015)].
[6] K. Agashe, A. Delgado, M. J. May, and R. Sundrum, J. High Energy Phys. 08 (2003) 050.
[7] R. Contino, L. Da Rold, and A. Pomarol, Phys. Rev. D **75**, 055014 (2007).
[8] S. Gopalakrishna, T. Mandal, S. Mitra, and G. Moreau, J. High Energy Phys. 08 (2014) 079.
[9] H. q. Zheng, Phys. Lett. B **378**, 201 (1996); **382**, 448(E) (1996).
[10] B. Patt and F. Wilczek, arXiv:hep-ph/0605188.
[11] S. Gopalakrishna, S. J. Lee, and J. D. Wells, Phys. Lett. B **680**, 88 (2009).
[12] S. Baek, P. Ko, and W. I. Park, J. High Energy Phys. 02 (2012) 047.
[13] A. Aravind, M. Xiao, and J. H. Yu, Phys. Rev. D **93**, 123513 (2016); **96**, 069901 (2017).
[14] Q. Lu, D. E. Morrissey, and A. M. Wijangco, J. High Energy Phys. 06 (2017) 138.
[15] R. Dermisek, Phys. Rev. D **87**, 055008 (2013).
[16] B. Bhattacherjee, P. Byakti, A. Kushwaha, and S. K. Vempati, J. High Energy Phys. 05 (2018) 090.
[17] D. Emmanuel-Costa and R. Gonzalez Felipe, Phys. Lett. B **623**, 111 (2005).
[18] V. Barger, J. Jiang, P. Langacker, and T. Li, Int. J. Mod. Phys. A **22**, 6203 (2007).

[19] I. Dorsner, S. Fajfer, and I. Mustac, Phys. Rev. D **89**, 115004 (2014).
[20] W. Chao, J. H. Zhang, and Y. Zhang, J. High Energy Phys. 06 (2013) 039.
[21] I. Masina, Phys. Rev. D **87**, 053001 (2013).
[22] A. Kobakhidze and A. Spencer-Smith, J. High Energy Phys. 08 (2013) 036.
[23] R. N. Mohapatra and Y. Zhang, J. High Energy Phys. 06 (2014) 072.
[24] L. Delle Rose, C. Marzo, and A. Urbano, J. High Energy Phys. 12 (2015) 050.
[25] S. Goswami, K. N. Vishnudath, and N. Khan, Phys. Rev. D **99**, 075012 (2019).
[26] A. Datta and S. Raychaudhuri, Phys. Rev. D **87**, 035018 (2013).
[27] L. A. Anchordoqui, I. Antoniadis, H. Goldberg, X. Huang, D. Lust, T. R. Taylor, and B. Vlcek, J. High Energy Phys. 02 (2013) 074.
[28] C. Coriano, L. Delle Rose, and C. Marzo, Phys. Lett. B **738**, 13 (2014).
[29] C. Coriano, L. Delle Rose, and C. Marzo, J. High Energy Phys. 02 (2016) 135.
[30] E. Accomando, C. Coriano, L. Delle Rose, J. Fiaschi, C. Marzo, and S. Moretti, J. High Energy Phys. 07 (2016) 086.
[31] J. Elias-Miro, J. R. Espinosa, G. F. Giudice, H. M. Lee, and A. Strumia, J. High Energy Phys. 06 (2012) 031.
[32] O. Lebedev, Eur. Phys. J. C **72**, 2058 (2012).
[33] A. Joglekar, P. Schwaller, and C. E. M. Wagner, J. High Energy Phys. 12 (2012) 064.
[34] Y. Hamada, H. Kawai, and K. y. Oda, J. High Energy Phys. 07 (2014) 026.
[35] N. Haba, H. Ishida, R. Takahashi, and Y. Yamaguchi, J. High Energy Phys. 02 (2016) 058.
[36] A. Kobakhidze and A. Spencer-Smith, Phys. Lett. B **722**, 130 (2013).
[37] A. Kobakhidze and A. Spencer-Smith, arXiv:1404.4709.
[38] W. Chao, M. Gonderinger, and M. J. Ramsey-Musolf, Phys. Rev. D **86**, 113017 (2012).
[39] W. Altmannshofer, M. Bauer, and M. Carena, J. High Energy Phys. 01 (2014) 060.
[40] M. L. Xiao and J. H. Yu, Phys. Rev. D **90**, 014007 (2014); **90**, 019901 (2014).
[41] S. Weinberg, *The Quantum Theory of Fields. Vol. 2: Modern Applications* (Cambridge University Press, Cambridge, England, 1995).
[42] S. A. R. Ellis, R. M. Godbole, S. Gopalakrishna, and J. D. Wells, J. High Energy Phys. 09 (2014) 130.
[43] F. Staub, arXiv:0806.0538.
[44] F. Staub, Comput. Phys. Commun. **185**, 1773 (2014).
[45] S. Coleman, *Aspects of Symmetry: Selected Erice Lectures* (Cambridge University Press, Cambridge, England, 1985).
[46] S. R. Coleman, V. Glaser, and A. Martin, Commun. Math. Phys. **58**, 211 (1978).
[47] S. Gopalakrishna and T. S. Mukherjee, Adv. High Energy Phys. **2017**, 1 (2017).
[48] K. M. Lee and E. J. Weinberg, Nucl. Phys. **B267**, 181 (1986).
[49] P. B. Arnold, Phys. Rev. D **40**, 613 (1989).
[50] T. P. Cheng, E. Eichten, and L. F. Li, Phys. Rev. D **9**, 2259 (1974).
[51] L. N. Mihaila, J. Salomon, and M. Steinhauser, Phys. Rev. Lett. **108**, 151602 (2012).